

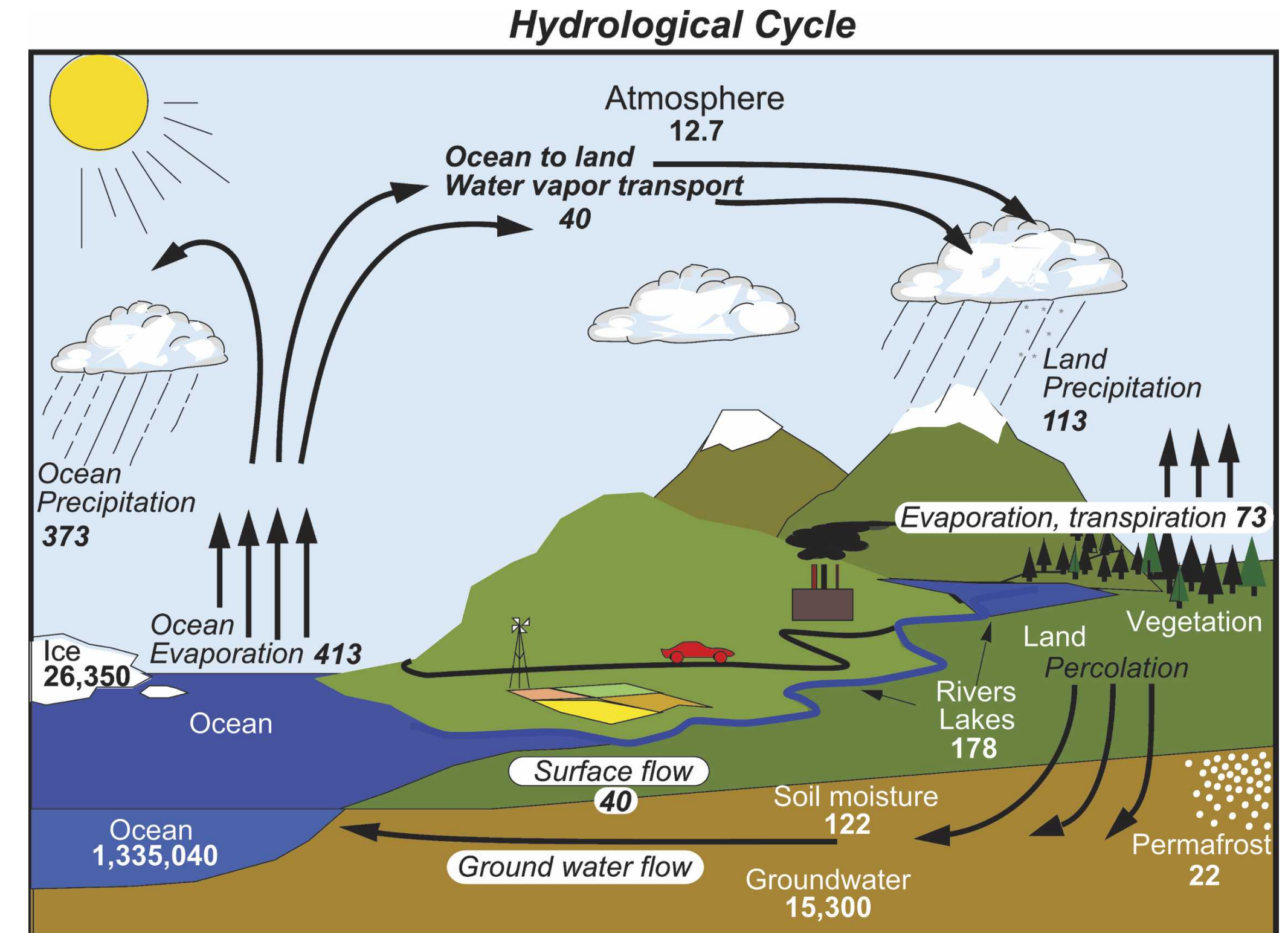
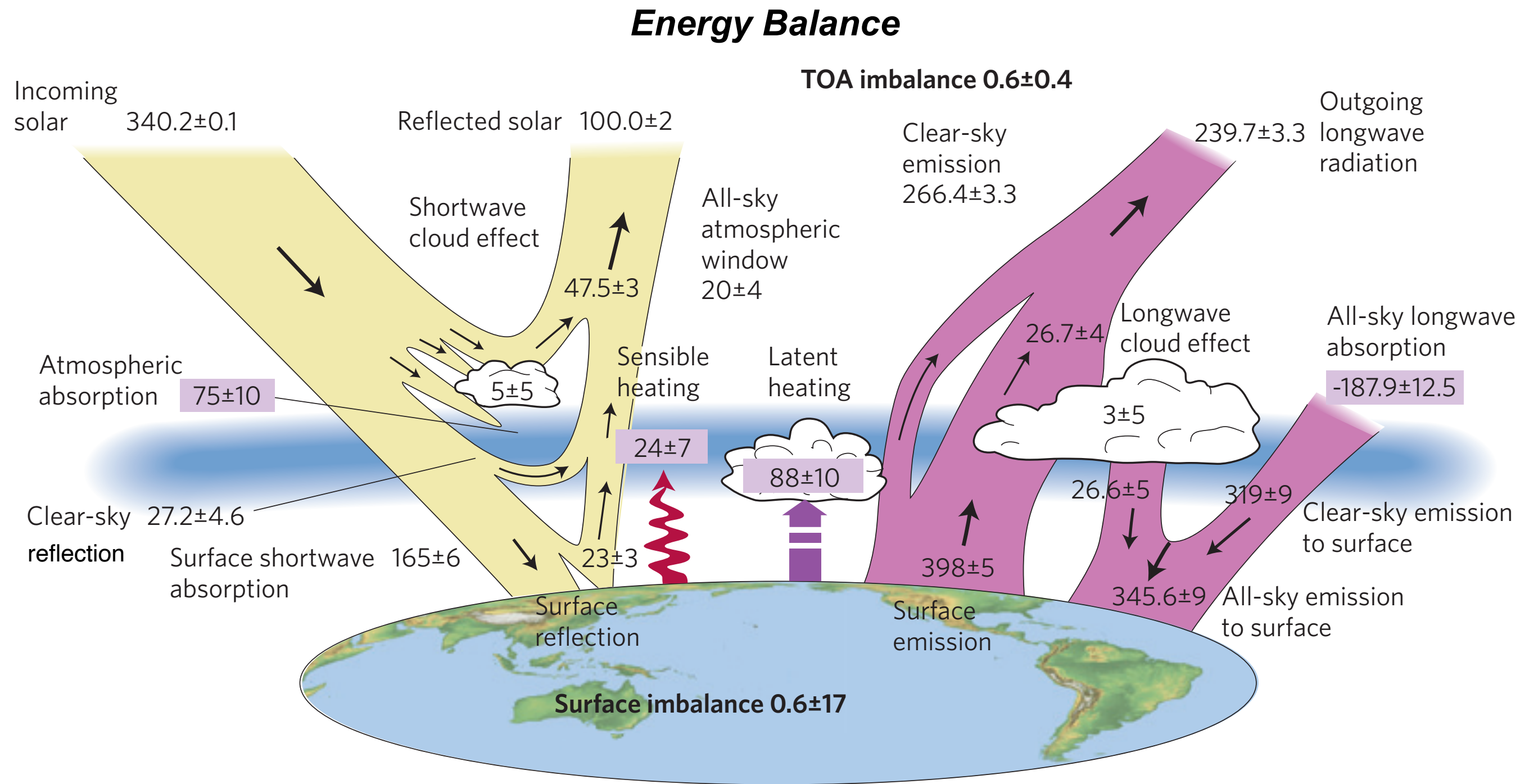
Advances in GFDL Microphysics for Cross-Scale Predictions

Linjong Zhou and the GFDL FV3 Team

Acknowledgments: our former leader S.-J. Lin, and our partners at NOAA and AI2

UFS S2S AT All-Hands, 5/12/2023

The Importance of Clouds



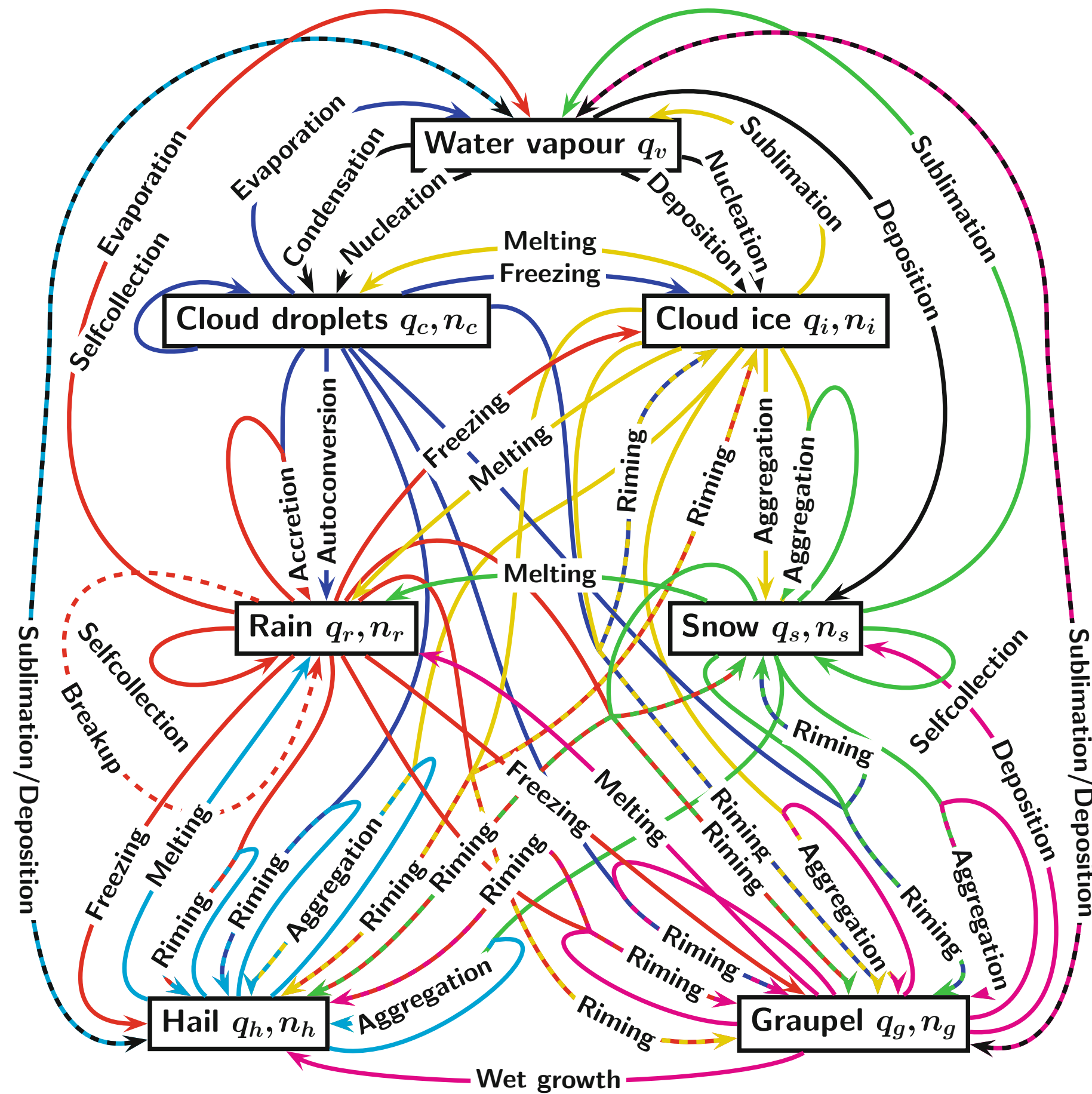
The global annual mean energy budget of Earth for the approximate period 2000-2010. (Stephens et al. 2012)

The hydrological cycle. (Trenberth et al. 2007)

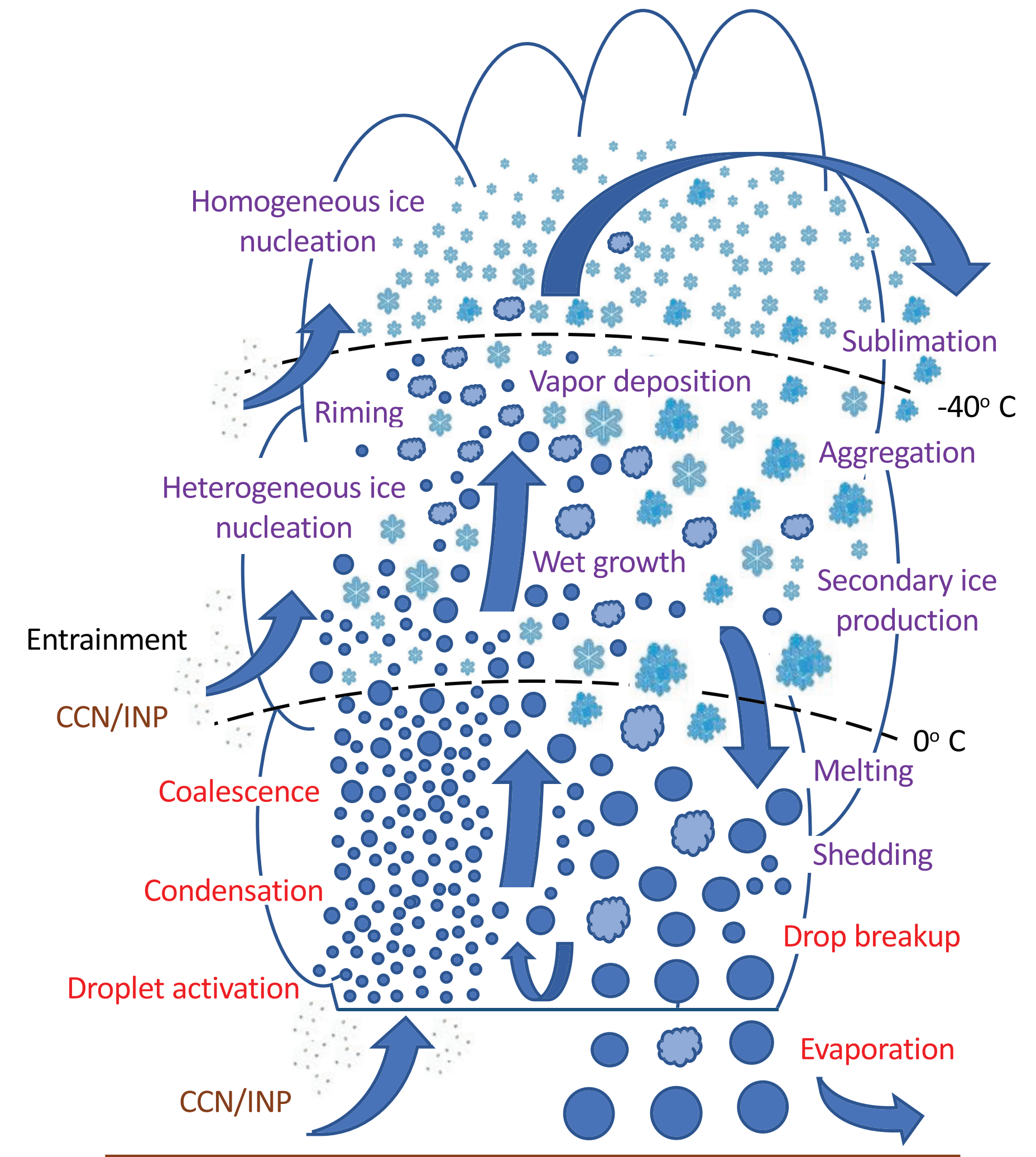
Cloud albedo effect (shortwave): $47.5 \pm 3 Wm^{-2}$
 Greenhouse effect (longwave): $26.4 \pm 4 Wm^{-2}$
 Net loss of radiation from Earth by clouds: $21.1 \pm 5 Wm^{-2}$

Cloud is the carrier of water.

The Complexity of Cloud Physics

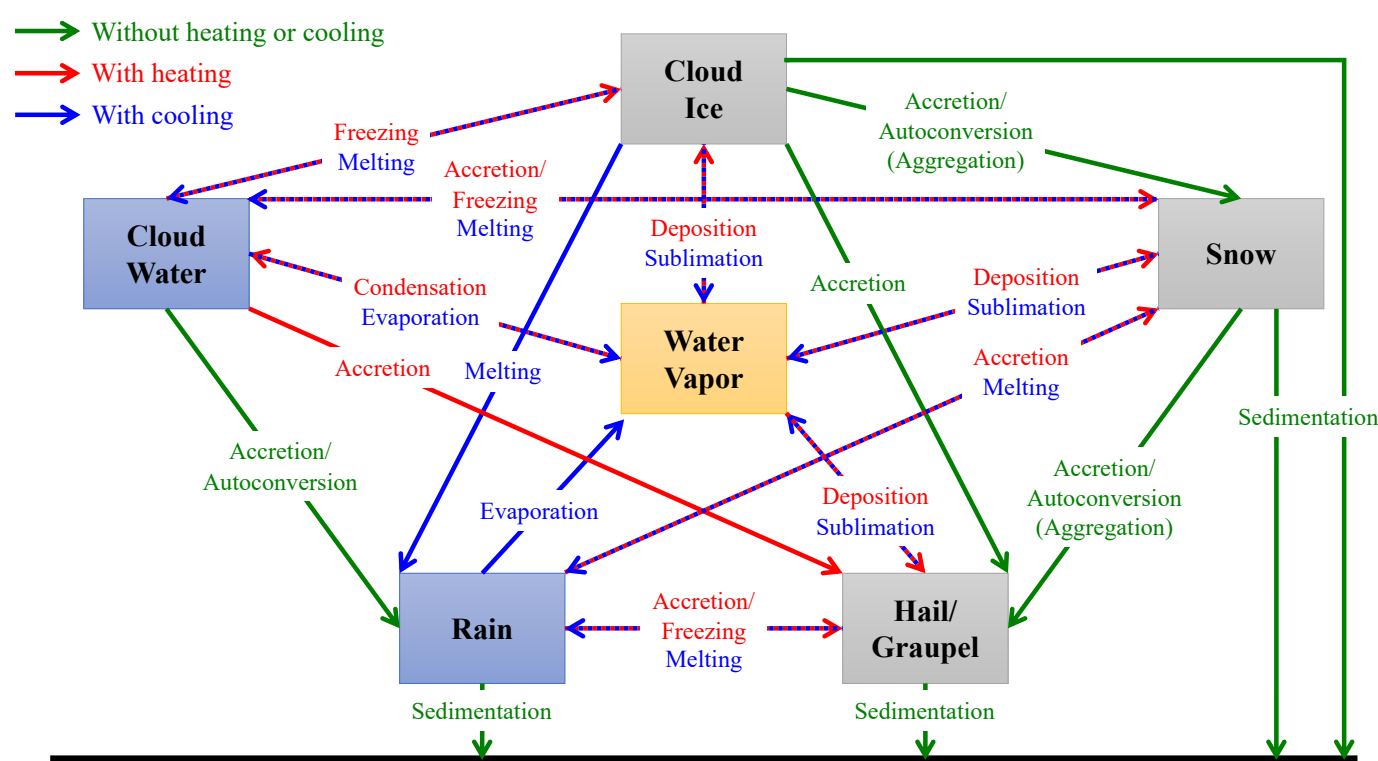


Schematic diagram of processes in the **six-class, 2-moment microphysics scheme of Seifert and Behang (2001)**. Figure courtesy of Axel Seifert. (Gettelman et al. 2019)



Schematic illustration of **microphysical processes within a typical cumulonimbus cloud**, highlighting the complexity of microphysics in the atmosphere. (Morrison et al. 2020)

GFDL current-generation model configurations



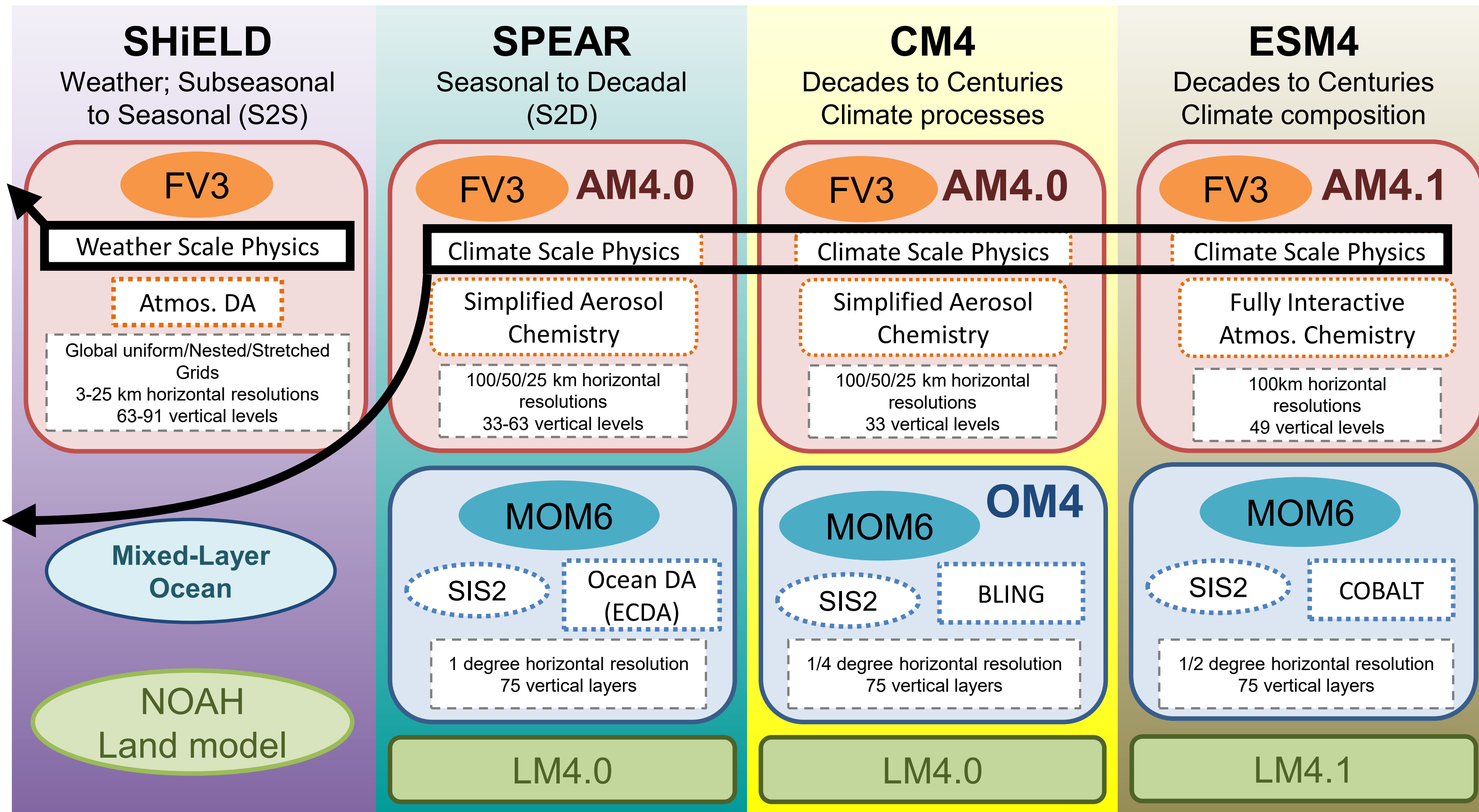
Zhou et al. 2019, Harris et al. 2020, Zhou et al. 2022

GFDL Microphysics for weather to seasonal scale prediction

AM4-MG2	
microphysics	two-moment Morrison-Gottelman with prognostic precipitation (MG2) (Gottelman & Morrison, 2015)
^b drop activation	mechanistic (Ming et al., 2006, 2007)
ice nucleation	dust and temperature-dependent for prognostic ice number concentration (Fan et al., 2019)

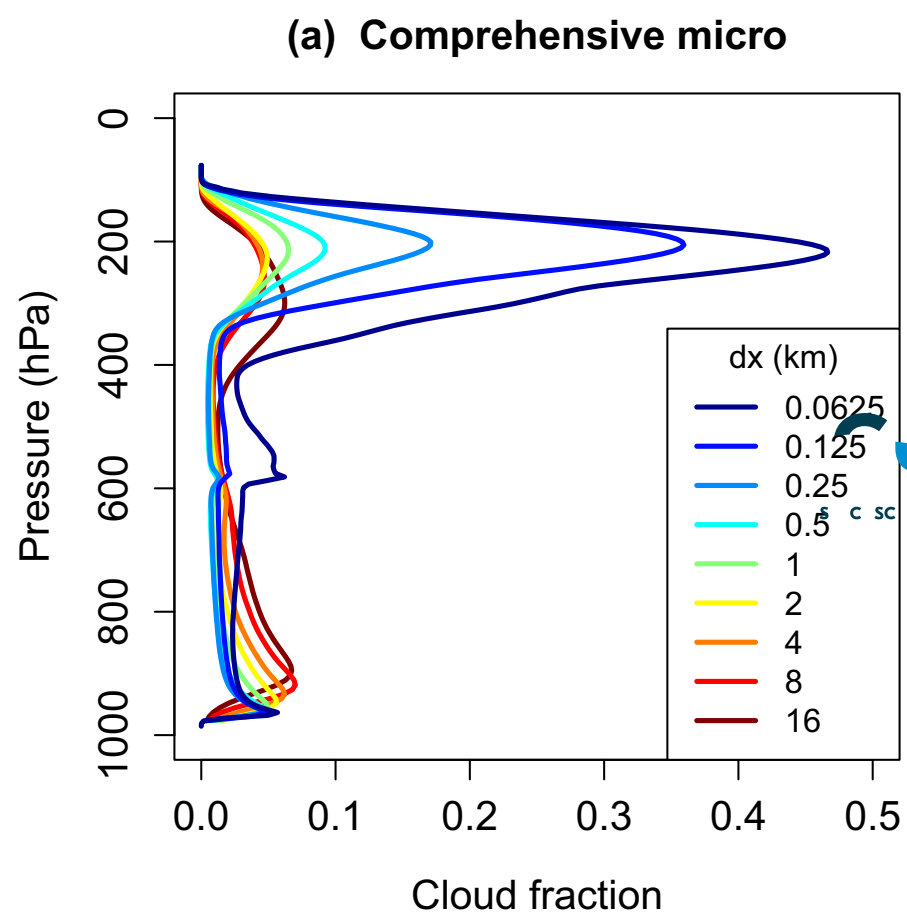
Guo et al. 2021, 2022

Revised MG2 Microphysics for seasonal to climate prediction and simulation

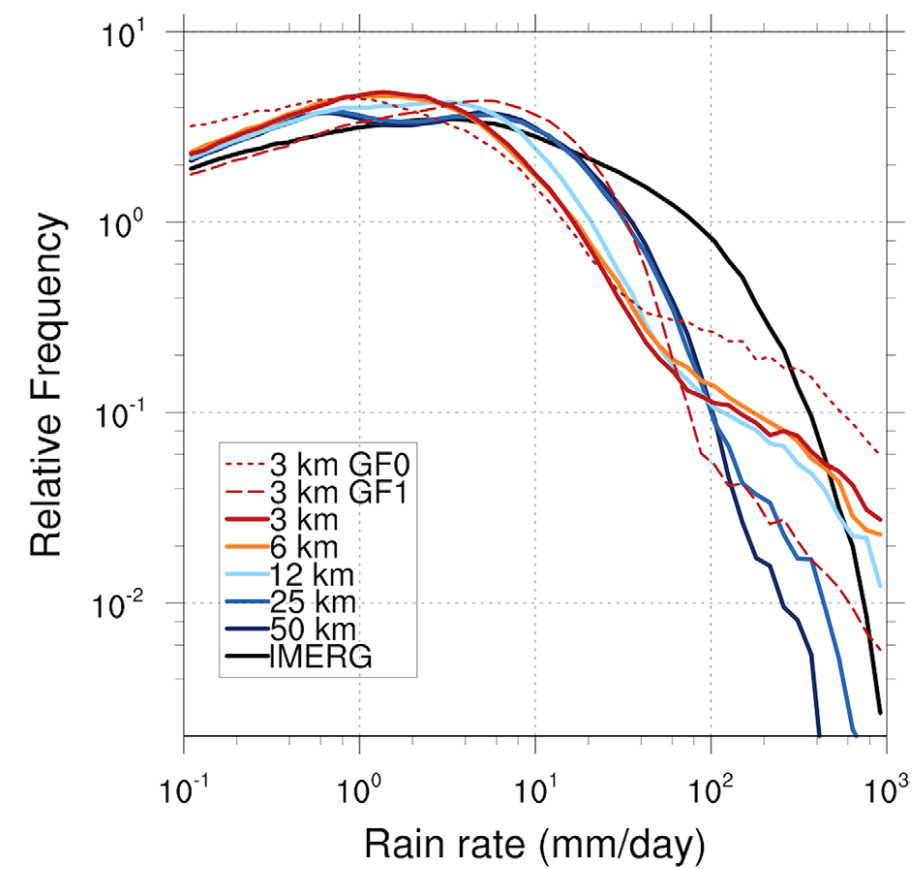


GFDL Microphysics Development at GFDL

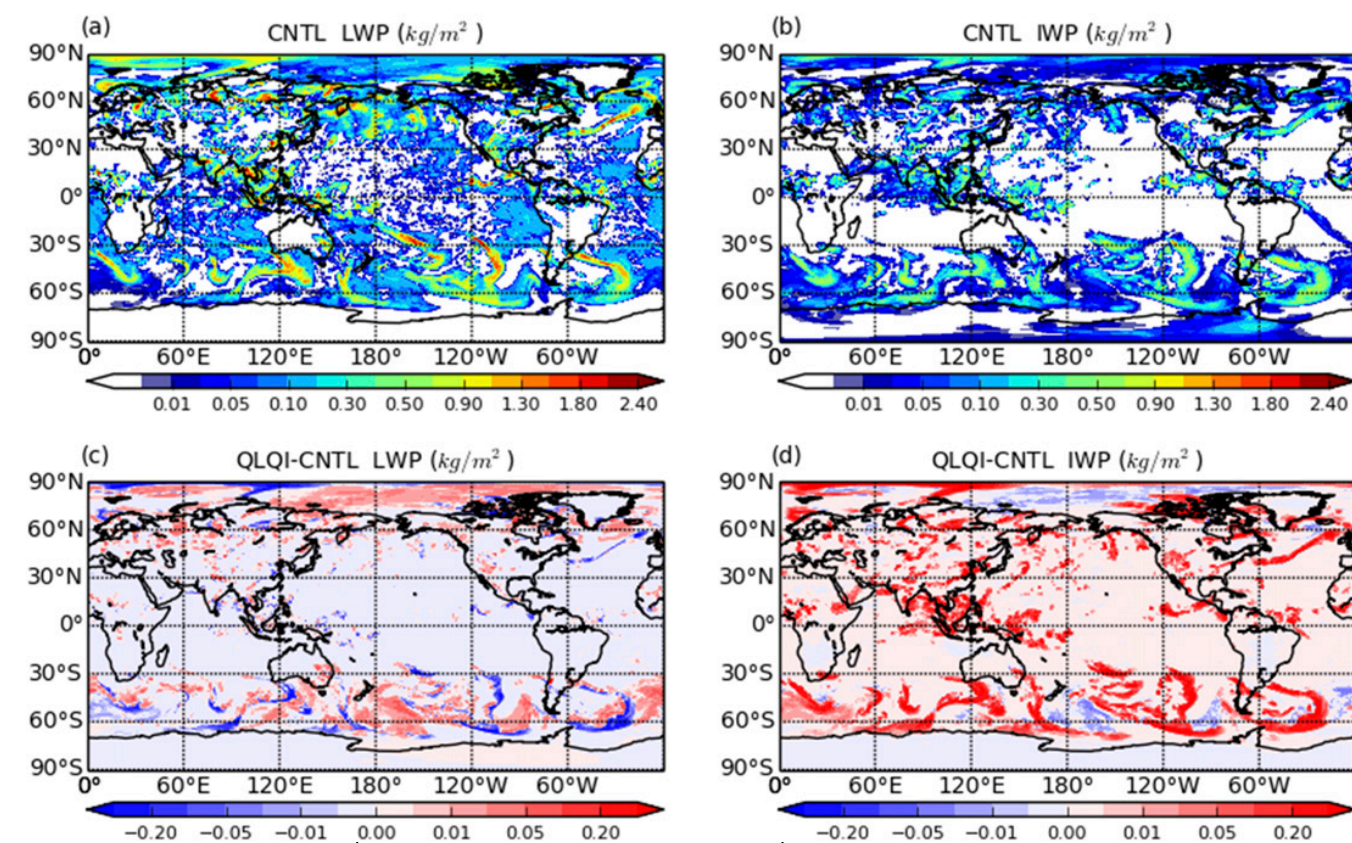
- **GFDL MP v0** (before 2015): **HiRAM** (Chen and Lin 2011, 2013)
 - Completely rewrote from Lin MP from GFDL ZETAC
- **GFDL MP v1** (2015-2017): *split MP*, **fvGFS/GFS/GEFS/UFS** (Zhou et al. 2019)
 - Developed for weather and convective-scale predictions
- **GFDL MP v2** (2017-2019): *inline MP*, **SHIELD 2020** (Harris et al. 2020)
 - Fully inline microphysics, advanced dynamics-physics coupling
- **GFDL MP v3** (2019-present): **SHIELD 2022** (Zhou et al. 2022)
 - Advances in microphysics foundation and processes



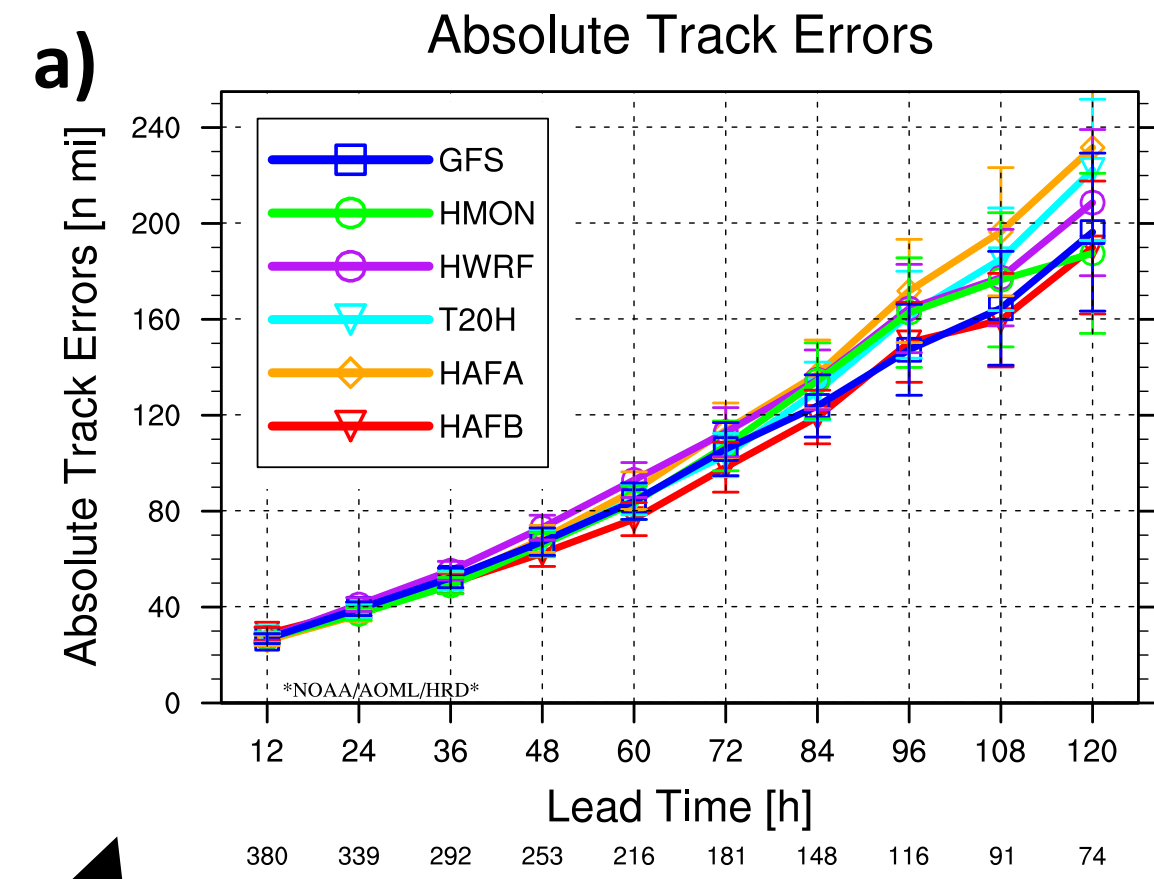
GFDL RCE: turbulence, convection, cloud, and cloud feedback (Jeevanjee 2017, Jeevanjee and Zhou 2022, Jeevanjee 2022)



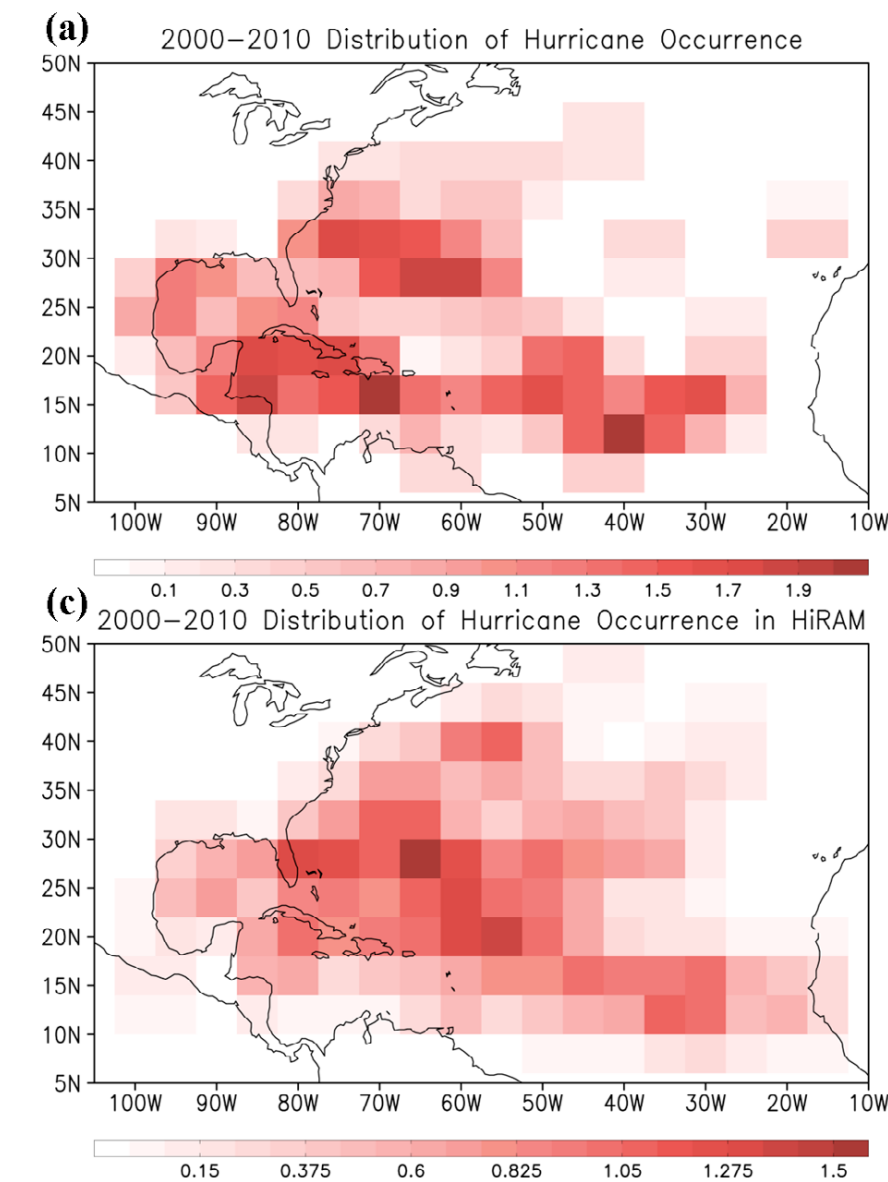
NASA: GEOS-5: global storm-scale modeling (Arnold et al. 2020)



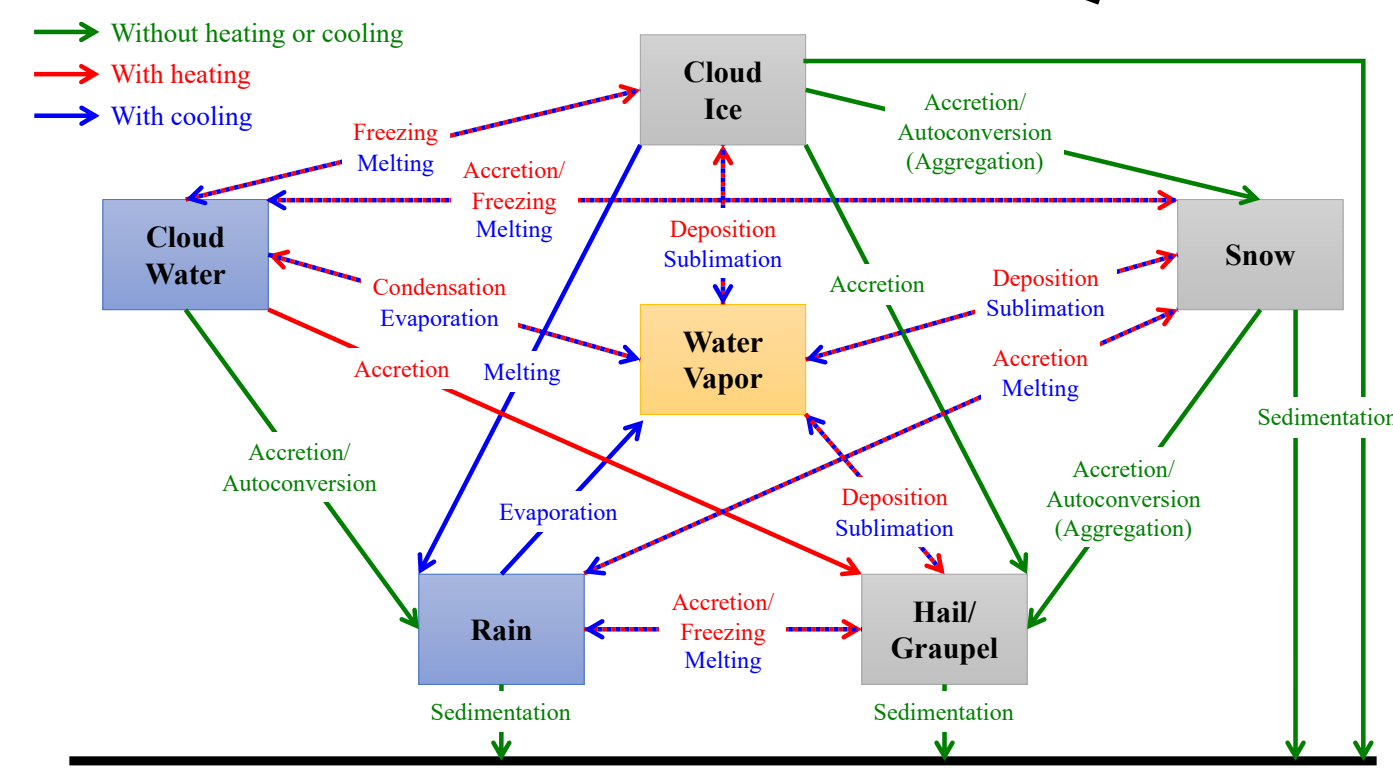
NWS GFS/GEFS: weather forecasts (Tong et al. 2020, Huang et al. 2021, Patel et al. 2021, ...)



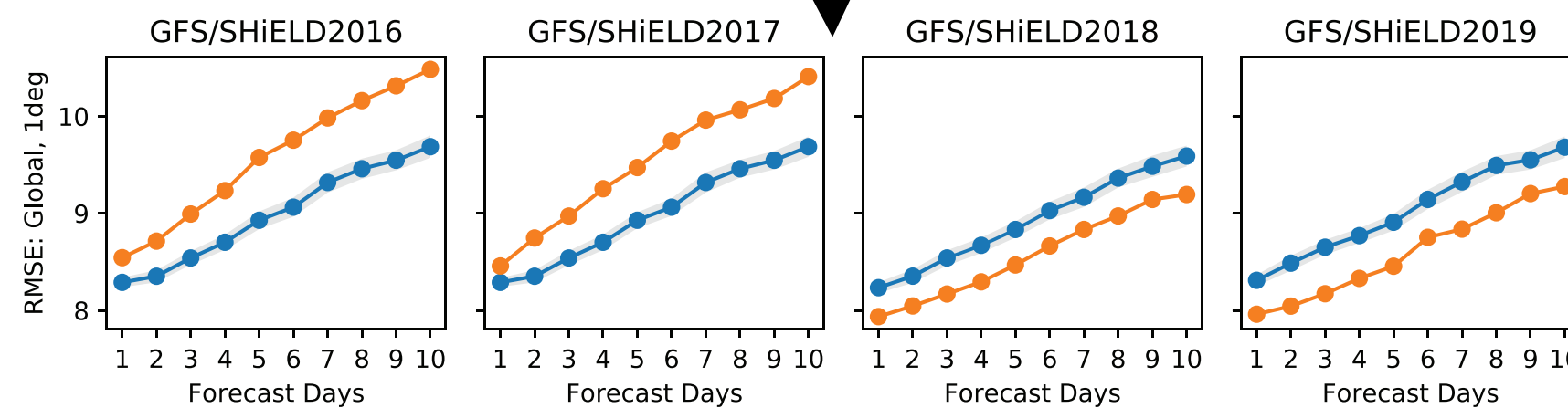
NWS HAFS: hurricane predictions (Dong et al. 2020, Hazelton et al. 2020, 2021, ...)



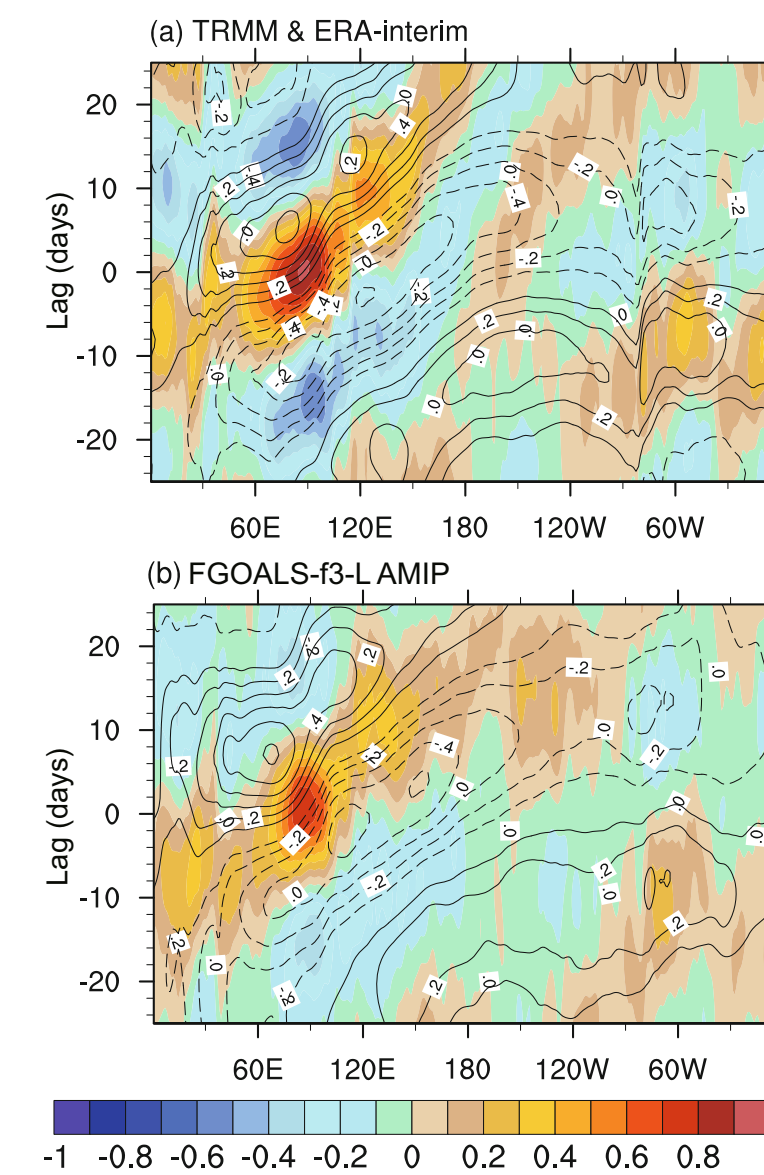
GFDL HiRAM: seasonal predictions and climate simulation (Chen and Lin 2011, 2013, Harris et al. 2016, Gao et al. 2017, 2019)



GFDL Microphysics (Zhou et al. 2010, Harris et al. 2020, Zhou et al. 2022)

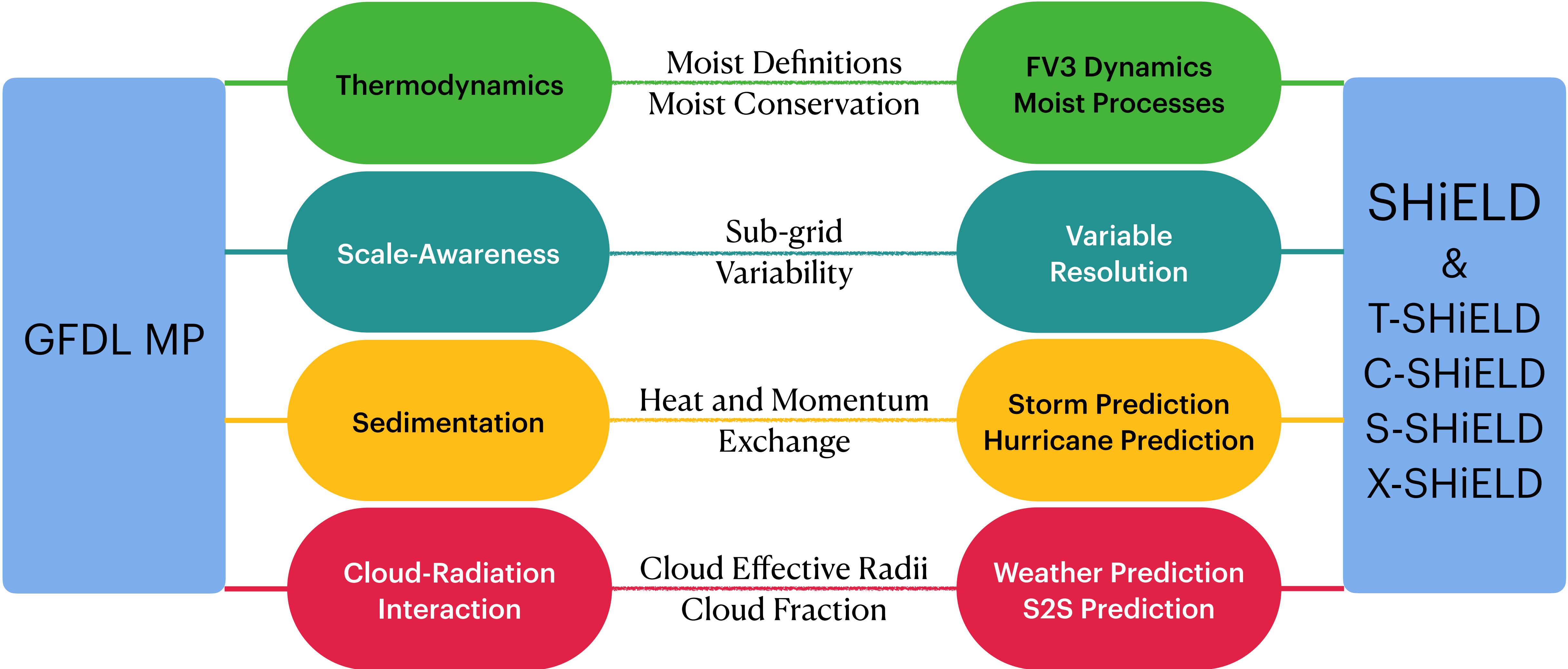


GFDL SHIELD: convective-scale predictions, weather forecast, sub-seasonal-to-seasonal predictions (Zhou et al. 2019, Chen et al. 2019, Harris et al. 2019, 2020, ...)

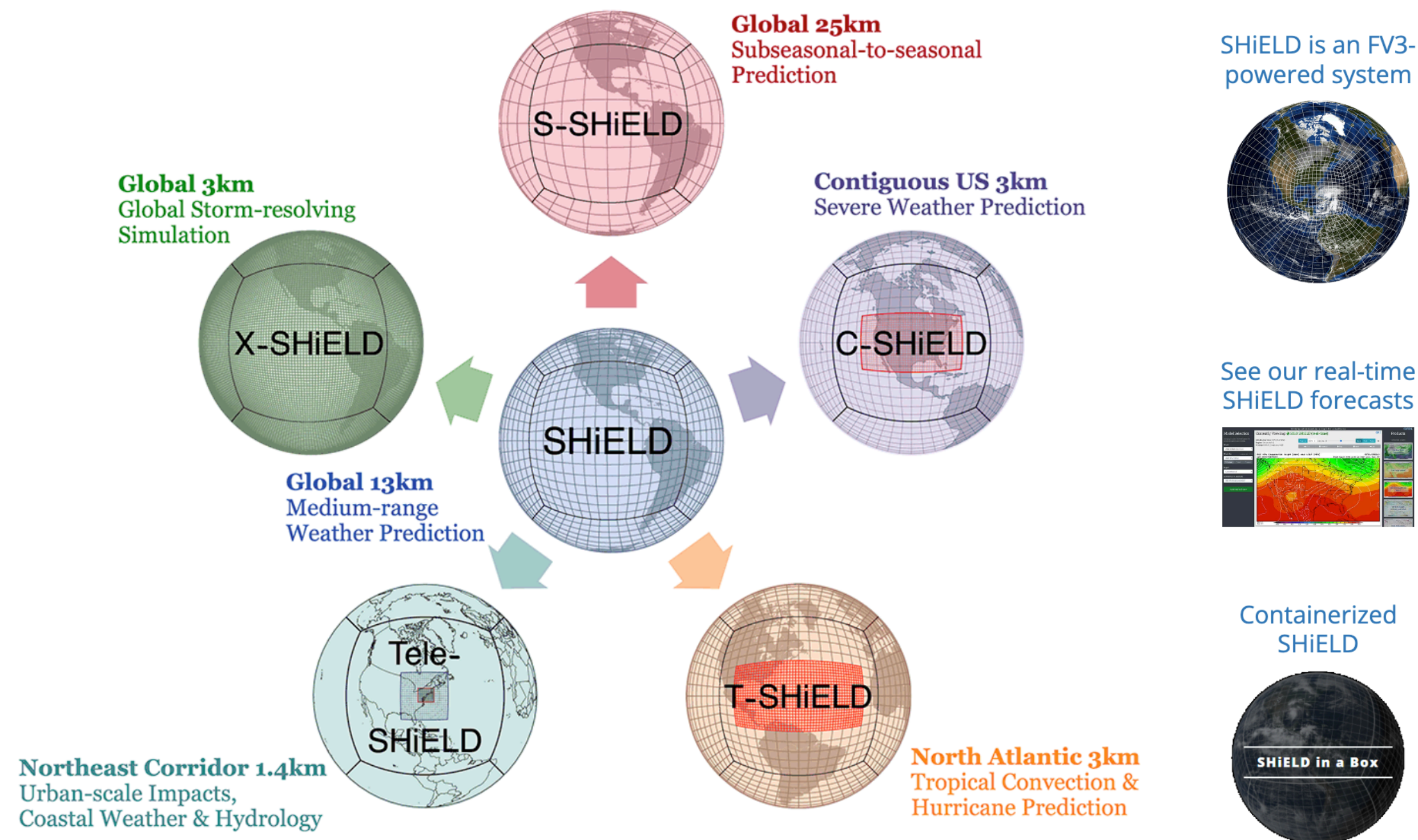


IAP FGOALS: seasonal predictions and climate simulation (Zhou et al. 2015; Li et al. 2017; He et al. 2019, 2020, 2021, ...)

GFDL MP for SHiELD Seamless Prediction



SHiELD System for High-resolution prediction on Earth-to-Local Domains



SHiELD is a Unified Forecast System (UFS) prototype atmosphere model showing the power of a unified prediction system across a variety of time and space scales designed for a wide array of applications. Homepage: <https://www.gfdl.noaa.gov/shield/> (Harris et al. 2020)

Configuration	Use	Domain	Integration Length
SHiELD	Medium-range weather prediction	Global 13-km with 91 vertical levels	240 hours (10 days)
C-SHiELD	Short-to-medium-range contiguous US severe weather prediction	Global 13-km, 3-km CONUS nest, 63 vertical levels	126 hours (5.25 days)
T-SHiELD	Medium-range Atlantic tropical cyclone and hurricane prediction	Global 13-km, 3.5-km tropical Atlantic nest, 63 vertical levels	168 hours (7 days), hurricane season only
S-SHiELD	Subseasonal-to-seasonal prediction	Global 25-km with 91 vertical levels	30 to 90 days, with up to 10 ensemble members
X-SHiELD	eXperimental DYAMOND-class global storm-resolving model (GSRM)	Global 3.25-km with 79 vertical levels	40 days
R-SHiELD	Regional limited-area model (LAM) configuration	Regional 13, 3, or 1 km	54 hours
Tele-SHiELD	Short-to-medium-range severe weather prediction, urban-scale impacts, coastal weather and hydrology, sub-grid scale land-use variability	Global 13-km, 4.3-km first nest, 1.4-km second nest for Northeast Corridor areas, 91 vertical levels	240 hours (10 days)

#1 Time Scales of Dynamics and Physics

Dynamical Core

Physical Parameterizations

Model	Dynamics	Turbulent Diffusion	Convection	Cloud and Precipitation	Orographic Subgrid Drag	Radiation	Surface Exchange
UM ¹	Fast	Fast	Fast	Fast + Slow	Slow	Slow	Fast
IFS ²	Fast	Fast	Fast + Slow	Fast + Slow	Fast	Slow	Fast
SHiELD ³	Fast	Fast	Intermediate	Intermediate	Fast	Slow	Fast

¹ Walters et al. (2017) based on Met Office UM

² Beljaars et al. (2018) based on ECMWF IFS

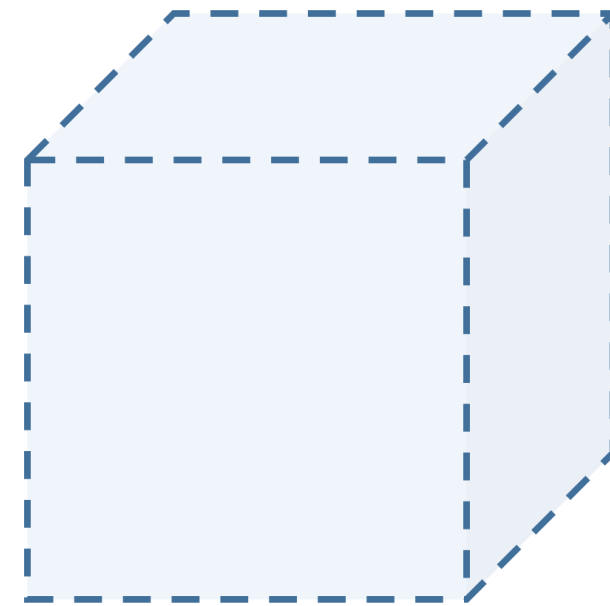
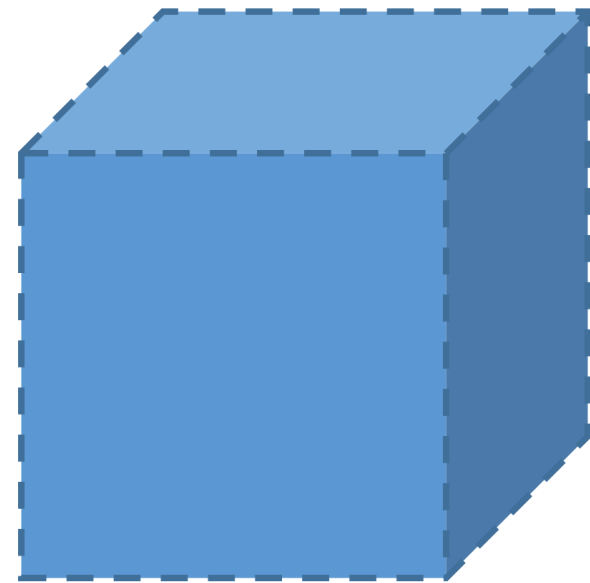
³ Zhou and Harris (2022) based on GFDL SHiELD

The concept of fast, intermediate, and slow are relative within each model.

#2 Thermodynamic Relationship

Dynamics: a Finite-Volume of moist air:

dry air + water vapor + liquid water + solid water



Heat Capacity	
dry air:	1004.6/717.56
water vapor:	1846/1410
liquid water:	4218
solid water:	2106

Physics: dry air + water vapor



Total Energy on Constant Volume

$$TE_m = c_v T + L_v q_v - L_f q_s + \Phi + K,$$

$$c_v = c_{vd} + q_v c_{vv} + q_l c_{vl} + q_s c_{vs},$$

$$L_v = L_{v0} - (c_{vv} - c_{vl}) T_0,$$

$$L_f = L_{f0} - (c_{vl} - c_{vs}) T_0.$$

Total Enthalpy on Constant Pressure

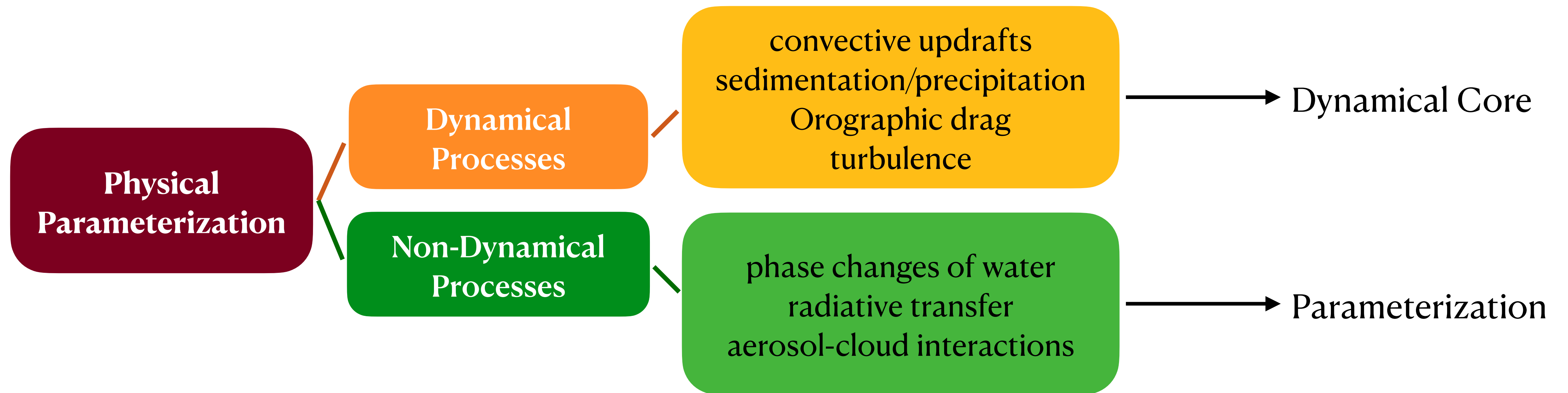
$$TE_d = c_{pd} T + L_{v0} q_v - L_{f0} q_s + \Phi + K,$$

Emanuel (1994), Satoh (2003), Harrop et al. (2022)

c_v is moist heat capacity and includes dry air c_{vd} , water vapor c_{vv} , liquid water c_{vl} , and solid water c_{vs} .

Latent heat coefficients (partly merged into $c_v T$) are functions of temperature derived from the Kirchhoff's equation.

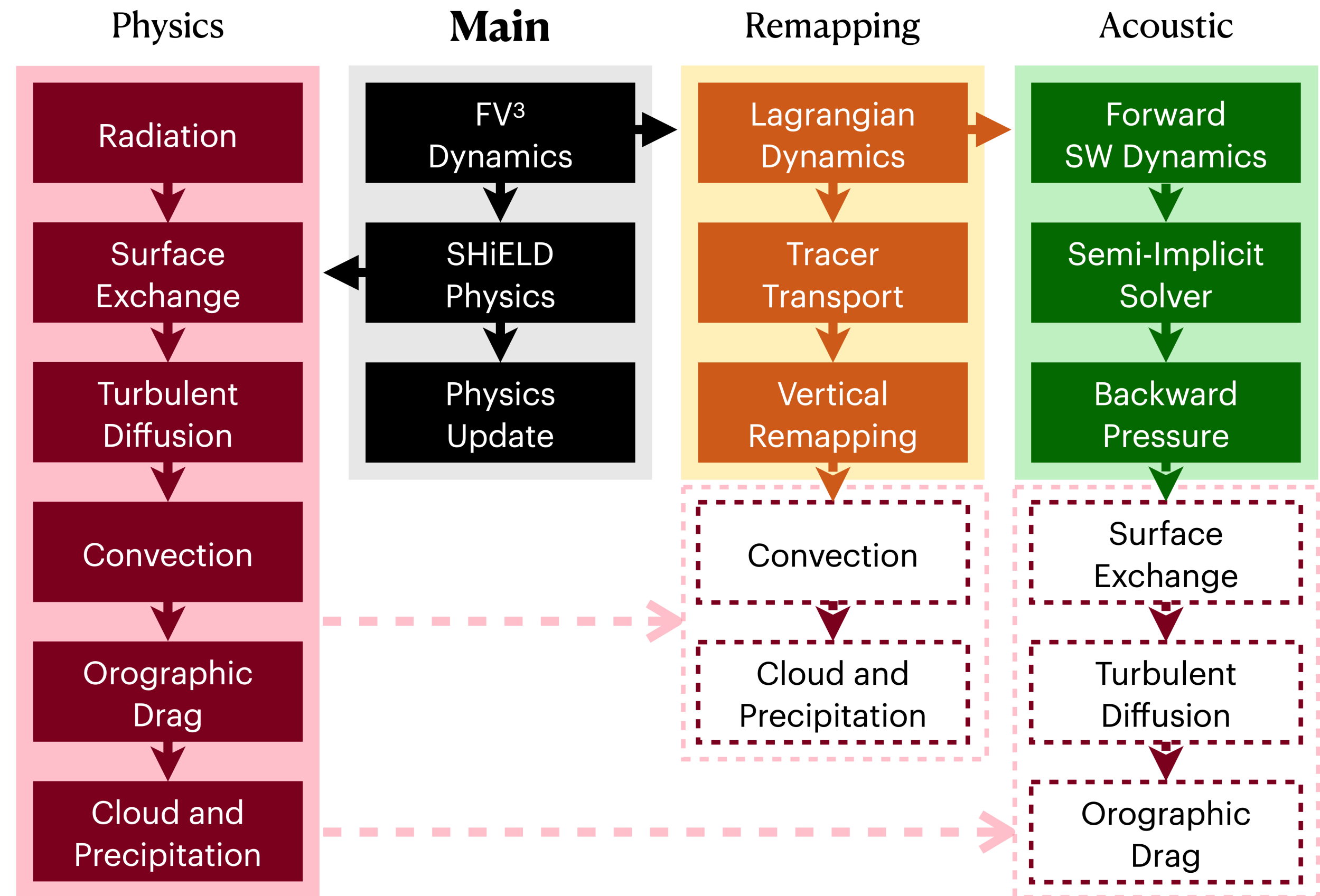
#3 Dynamical and Non-dynamical Processes



Dynamical processes, if resolved, should be taken care of by the dynamical core. Especially when the model's resolution reaches a few kilometers or less and deep convective updrafts can be explicitly represented.

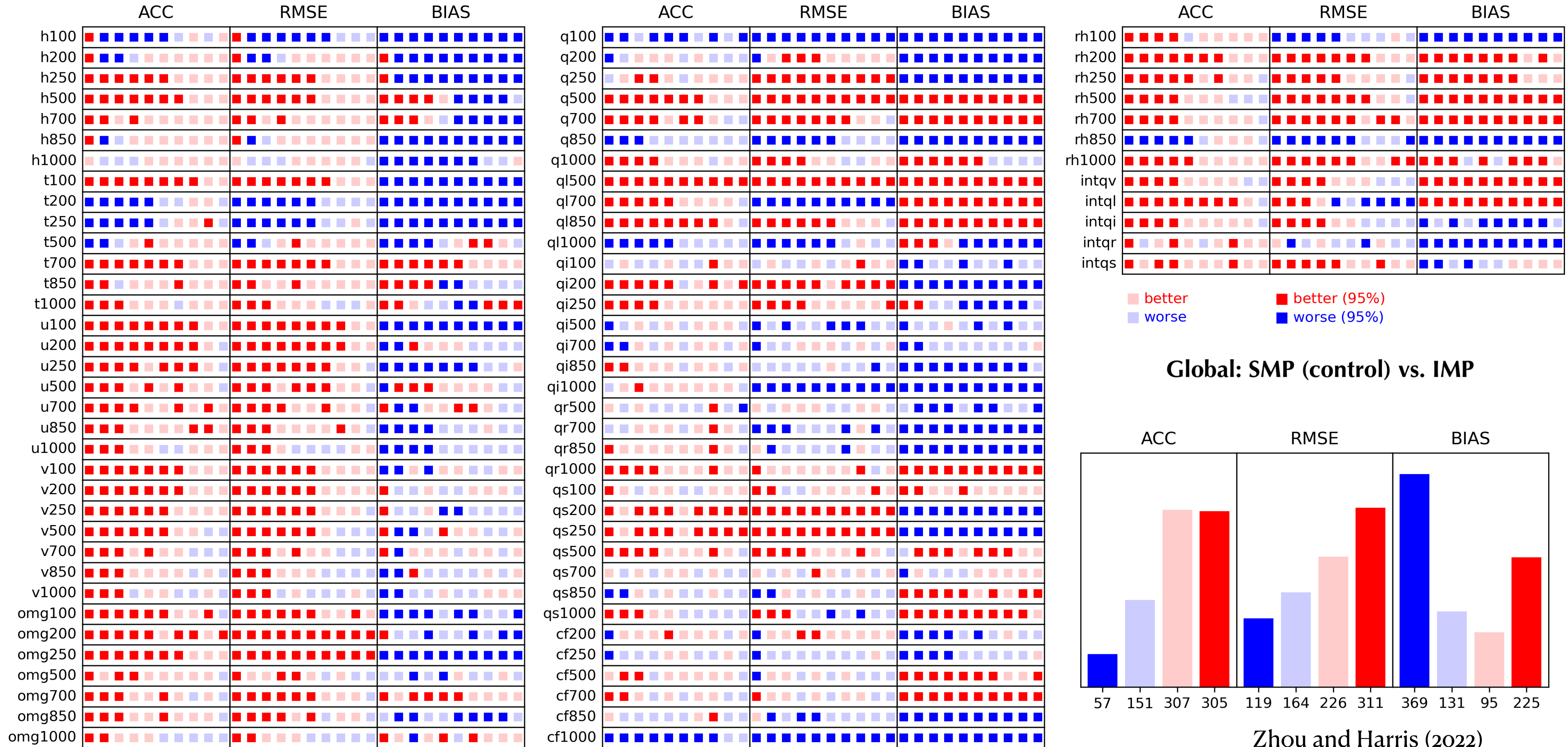
- **In the completed integrated framework**

- the surface exchange, turbulent diffusion, and orographic drag are relatively fast processes that would be moved from the physics loop into the acoustic loop.
- The convection and cloud and precipitation are intermediate-timescale processes that would be moved from the physics loop into the remapping loop.



Proposed schematic of the integrated dynamics-physics coupling framework in SHIELD — Zhou and Harris (2022)

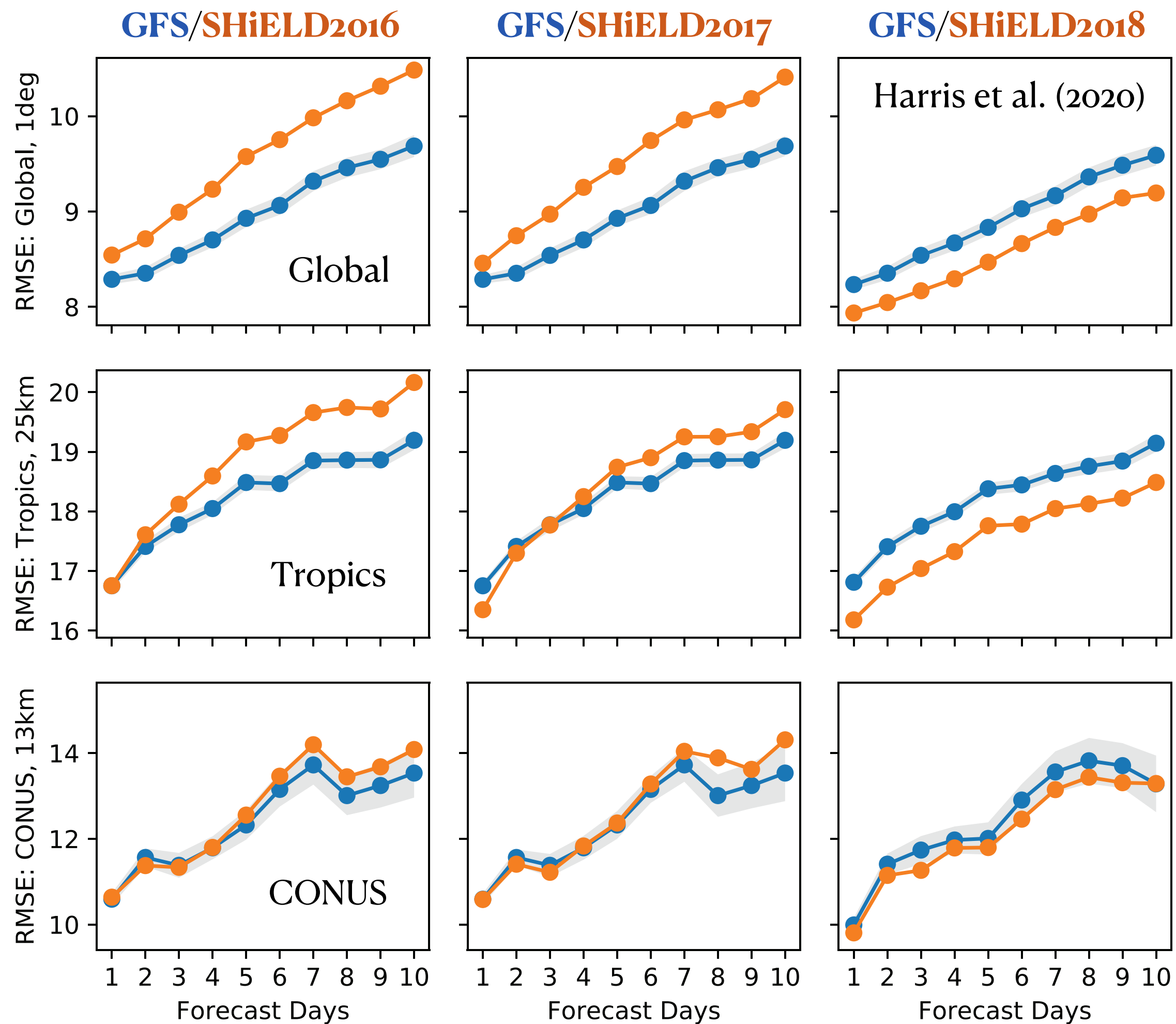
First successful example: moved the GFDL cloud microphysics into the FV3 dynamical core



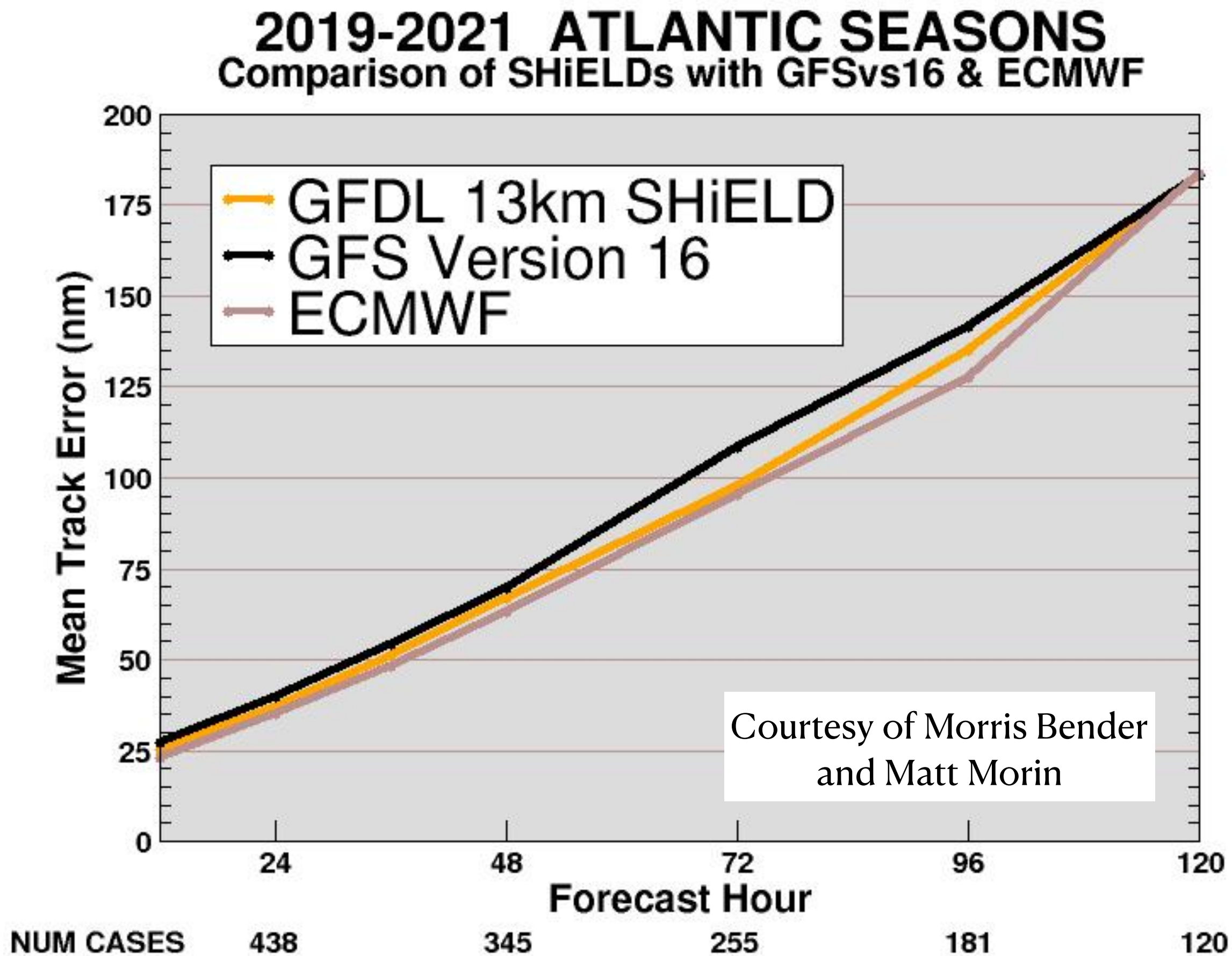
Red means better, blue means worse.

IMP yields significantly higher skill and lower error than the SMP in many meteorological fields. Geopotential height, temperature, wind, specific humidity, cloud et al.

SHiELD Predictions with GFDL MP and Integrated Coupling

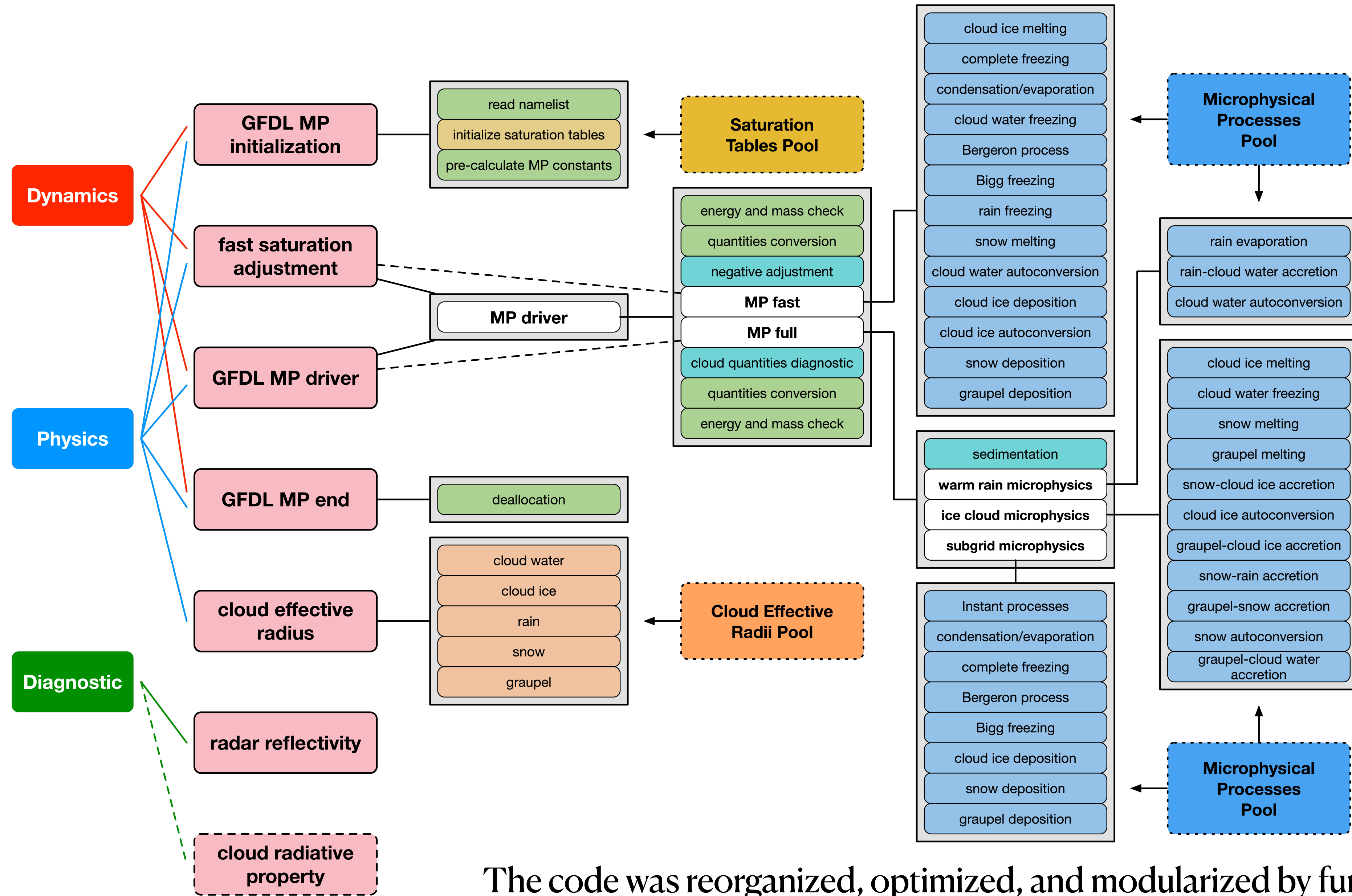


RMSE of Precipitation Prediction
 ZC MP → Split GFDL MP → Inline GFDL MP



Hurricane Prediction Track Error
 SHiELD: Inline GFDL MP
 GFS: Split GFDL MP

Major Updates in GFDL MP v3: #1 Code Reorganization



The code was reorganized, optimized, and modularized by functions.

Major Updates in GFDL MP v3: #2 Particle Size Distribution

- Mono-dispersed for cloud water and cloud ice
- Number concentrations are prescribed as constants
- Effective radii are diagnosed inconsistently
- Cloud water doesn't fall
- Cloud ice fall speed is diagnosed by temperature

Gamma Particle Size Distribution (PSD) for all cloud categories

$$n(D) = n_0 D^{\mu-1} \exp(-\lambda D)$$

Other quantities are derived naturally

$$N = \int_0^{\infty} n(D) dD = \frac{n_0 \Gamma(\mu)}{\lambda^\mu},$$

$$D_{\text{eff}} = \frac{\int_0^{\infty} D^3 n(D) dD}{\int_0^{\infty} D^2 n(D) dD} = \frac{\mu + 2}{\lambda},$$

$$\beta = \frac{\pi}{2} \int_0^{\infty} D^2 n(D) dD = \frac{\pi n_0 \Gamma(\mu + 2)}{2 \lambda^{\mu+2}},$$

$$q = \frac{\pi \rho_0}{6 \rho} \int_0^{\infty} D^3 n(D) dD = \frac{\pi \rho_0 n_0 \Gamma(\mu + 3)}{6 \rho \lambda^{\mu+3}},$$

$$Z = \int_0^{\infty} D^6 n(D) dD = \frac{n_0 \Gamma(\mu + 6)}{\lambda^{\mu+6}}.$$

Terminal velocities are also derived using PSD

$$V = \alpha D^\beta,$$

$$V_M = \frac{\int_0^{\infty} V D^3 n(D) dD}{\int_0^{\infty} D^3 n(D) dD} = \frac{\alpha \Gamma(\mu + \beta + 3)}{\lambda^\beta \Gamma(\mu + 3)},$$

Table 1

The Intercept Parameter (n_0 , Unit: $m^{-3-\mu}$), Spectral Shape Parameter (μ , Unit: 1), Density of Hydrometeor Category (ρ' , Unit: $kg m^{-3}$), Parameter α (Unit: $m^{1-\beta} s^{-1}$) and β for Each Hydrometeor Category of the GFDL MP v3

	Cloud water	Cloud ice	Rain	Snow	Graupel	Hail
n_0	1.2×10^{66}	1.1×10^{18}	8×10^6	3×10^6	4×10^6	4×10^4
μ	11	3.445	1	1	1	1
ρ'	1×10^3	9.17×10^2	1×10^3	1×10^2	4×10^2	9.17×10^2
α	3×10^7	7×10^2	842	4.8	40.74	61.68445
β	2	1	0.8	0.25	0.5	0.5
D_{eff}	10–20	20–300	20–20,000	300–20,000	300–20,000	300–20,000
V	0–0.01	0–1	0–12	0–2	0–12	0–12

Note. The valid ranges of effective diameter (D_{eff} , unit: $\times 10^{-6}$ m) and terminal velocity (V , unit: $m s^{-1}$) are at the bottom of this table. Parameters n_0 and μ for cloud water, cloud ice, rain, snow, and graupel or hail are derived based on Martin et al. (1994), Fu (1996), Marshall and Palmer (1948), Gunn and Marshall (1958), and Houze et al. (1979) or Federer and Waldvogel (1975), respectively. Parameters α and β for cloud water, cloud ice, rain, snow, and graupel or hail follow Ikawa and Saito (1991), McFarquhar et al. (2015), Liu and Orville (1969), Straka (2009), and Pruppacher and Klett (2010), respectively.

Zhou et al. (2022)

Major Updates in GFDL MP v3: #3 Microphysical Processes

Accretion (v2):

$$P_{xacy} = \frac{\pi E_{xy} n_{x0} \alpha_x q_y \Gamma(3 + \beta_x)}{4 \lambda^{3 + \beta_x}} \left(\frac{\rho_0}{\rho} \right)^{1/2}$$

$$P_{xacy} = \pi^2 E_{xy} n_{x0} n_{y0} |V_x - V_y| \frac{\rho_y}{\rho} \left(\frac{5}{\lambda_x \lambda_y^6} + \frac{0.5}{\lambda_x^3 \lambda_y^4} + \frac{2}{\lambda_x^2 \lambda_y^5} \right)$$

Accretion (v3):

$$P_{xacy} = \frac{\pi^2}{24} E_{xy} n_{x0} n_{y0} \sqrt{(\alpha V_x - \beta V_y)^2 + \gamma V_x V_y} \frac{\rho_y}{\rho} \left[\frac{\Gamma(\mu_x) \Gamma(\mu_y + 5)}{\lambda_x^{\mu_x} \lambda_y^{\mu_y + 5}} + \frac{\Gamma(\mu_x + 2) \Gamma(\mu_y + 3)}{\lambda_x^{\mu_x + 2} \lambda_y^{\mu_y + 3}} + \frac{2 \Gamma(\mu_x + 1) \Gamma(\mu_y + 4)}{\lambda_x^{\mu_x + 1} \lambda_y^{\mu_y + 4}} \right]$$

Evaporation, Sublimation, Deposition (v2):

$$P_{ESD} = \frac{2\pi (S - 1) n_0}{\rho (A + B)} \frac{n_0}{\lambda^2} V_f$$

$$V_f = 0.78 + 0.31 S_c^{1/3} \nu^{-1/2} \frac{\alpha^{1/2} \Gamma\left(\frac{\beta + 5}{2}\right)}{\lambda \frac{\beta + 5}{2}} \left(\frac{\rho_0}{\rho} \right)^{1/4} \lambda^2$$

Evaporation, Sublimation, Deposition (v3):

$$P_{ESD} = \frac{2\pi (S - 1) n_0 \Gamma(\mu + 1)}{\rho (A + B) \lambda^{\mu + 1}} V_f$$

$$V_f = 0.78 + 0.31 S_c^{1/3} \nu^{-1/2} \frac{\alpha^{1/2} \Gamma\left(\mu + \frac{\beta + 3}{2}\right)}{\lambda^{\mu + \frac{\beta + 3}{2}}} \left(\frac{\rho_0}{\rho} \right)^{1/4} \frac{\lambda^{\mu + 1}}{\Gamma(\mu + 1)}$$

Melting (v2):

$$P_{melt} = \frac{2\pi}{\rho L} [K_a T_c - L \psi \rho (q_s - q)] \frac{n_0}{\lambda^2} V_f$$

Melting (v3):

$$P_{melt} = \frac{2\pi}{\rho L} [K_a T_c - L \psi \rho (q_s - q)] \frac{n_0 \Gamma(\mu + 1)}{\lambda^{\mu + 1}} V_f$$

Rain Freezing (v2):

$$P_{gfr} = 20 \pi^2 n_0 \frac{\rho_w}{\rho} B' \exp [A' (T_0 - T) - 1] \lambda^{-7}$$

Rain Freezing (v3):

$$P_{gfr} = \frac{\pi^2}{36} n_0 \frac{\rho_w}{\rho} B' \exp [A' (T_0 - T) - 1] \frac{\Gamma(\mu + 6)}{\lambda^{\mu + 6}}$$

Major Updates in GFDL MP v3: #4 Aerosol-based CDNC

Cloud water to rain autoconversion (Manton and Cotton 1977):

$$P_{aut} = \frac{0.104g E_{aut} \rho^{4/3}}{\nu (N_c \rho')^{1/3}} q^{7/3} H(q - q_c),$$

$$q_c = \frac{N_c}{\rho} \frac{4}{3} \pi \rho' R_c^3.$$

Here, $E_{aut} = 0.5$ is the collection efficiency,

$\nu = 1.717 \times 10^{-5} \text{ m}^2 \text{ s}^{-1}$ is the dynamic viscosity of air,

$N_c \text{ (m}^{-3}\text{)}$ is the CDNC, $R_c = 10 \times 10^{-6} \text{ m}$ and $q_c \text{ (kg kg}^{-1}\text{)}$ are the critical mean cloud droplet radius and the mass mixing ratio respectively, and H is the Heaviside unit step function.

The species of sulfate, which is a subset of MERRA2 aerosol, is converted to CDNC using Boucher and Lohmann (1995)'s formula:

$$N_c = \begin{cases} 10^{2.24} (10^9 \rho q_a)^{0.257} \times 10^6 & \text{land,} \\ 10^{2.06} (10^9 \rho q_a)^{0.480} \times 10^6 & \text{ocean.} \end{cases}$$

Here, $q_a \text{ (kg kg}^{-1}\text{)}$ is the mass specific ratio of sulfate aerosol from MERRA2.

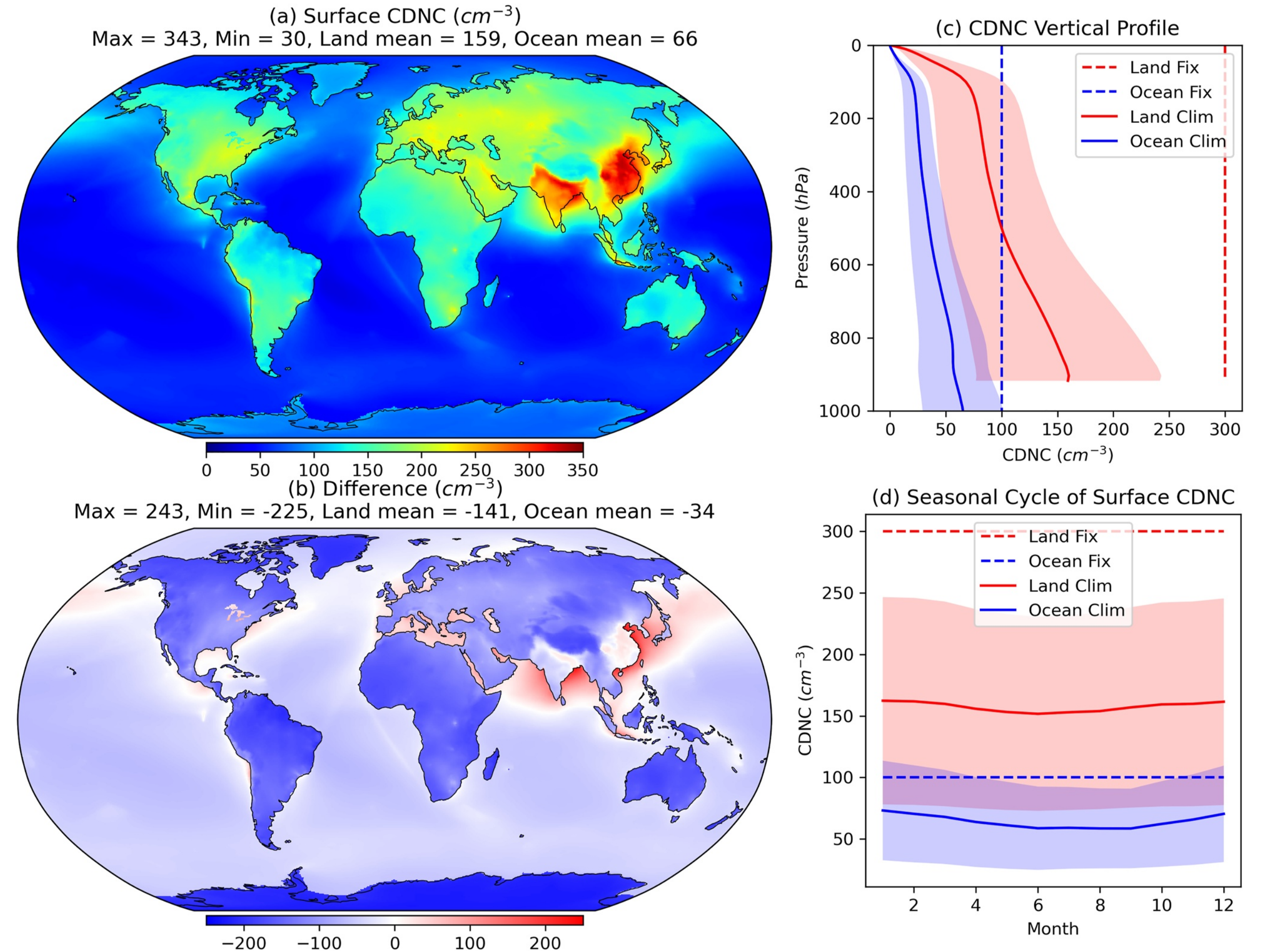
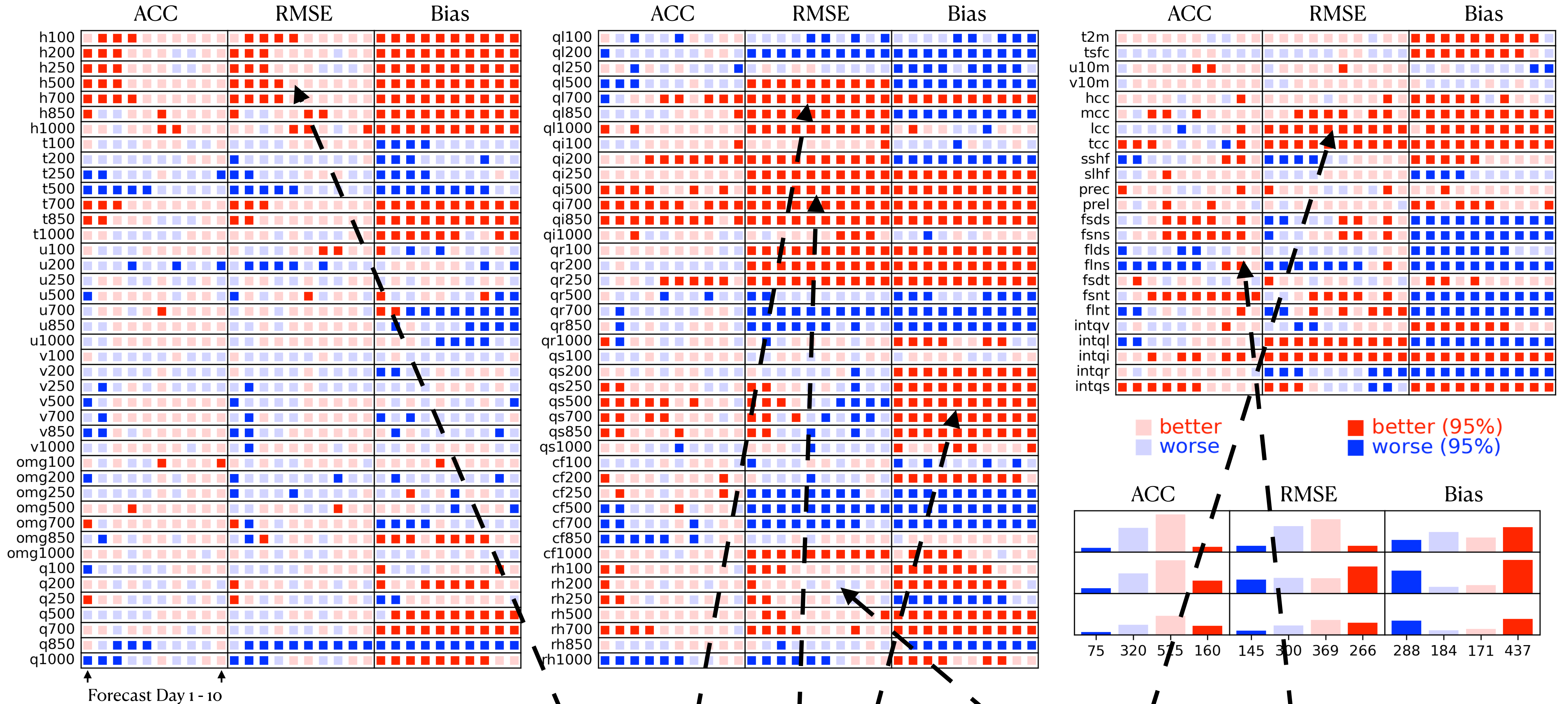


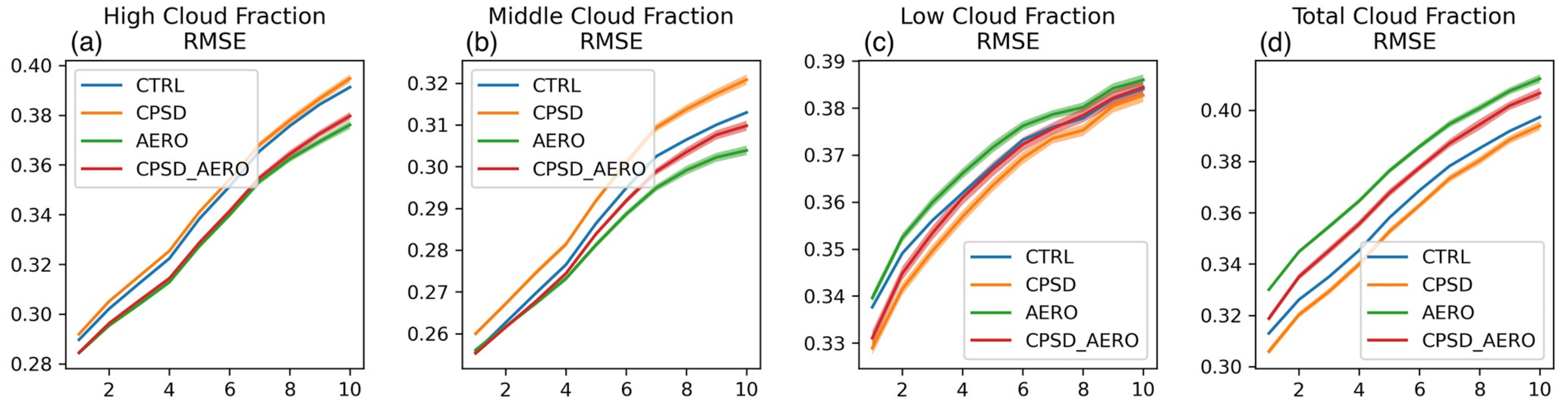
Figure 3. Geographic distribution of (a) surface climatological cloud droplet number concentration (CDNC) (cm^{-3}) calculated from Modern-Era Retrospective analysis for Research and Applications, version 2 (MERRA2), (b) the difference between the CDNC from MERRA2 and the fixed CDNC values used in the GFDL MP v2. Panel (c) is the vertical profiles of climatological CDNC from MERRA2 (solid) and fixed CDNC values used in the Geophysical Fluid Dynamics Laboratory cloud microphysics scheme (GFDL MP) v2 (dashed). Panel (d) is the seasonal cycle of climatological surface CDNC from MERRA2 (solid) and fixed CDNC values used in the GFDL MP v2 (dashed). Red lines represent CDNC in the land area, blue lines represent CDNC over the ocean. The shaded area is its standard deviation. The numbers in panels (a and b) are the global maximum, minimum, land mean, and ocean means of CDNC.

Scorecard, Large-scale Weather Prediction, GFDL MP v3 vs. v2 (reference)



Significant improvements: geopotential height, cloud water, cloud ice, snow, relative humidity, cloud fraction, radiative fluxes

Cloud Fraction Prediction: Sensitivity of PSD and Aerosol-based CDNC



- New PSD improves low and total cloud fraction prediction
- New CDNC improves middle and high cloud fraction prediction
- New PSD + new CDNC improves low, middle, and high cloud fraction prediction.

Table 2

List of Experiments in This Study

Experiment	New PSD ^a	New CDNC ^b	GFDL MP
CTRL			v3
CPSD	×		v3
AERO		×	v3
CPSD_AERO	×	×	v3

^agamma distribution for cloud water and exponential distribution for cloud ice. ^bCDNC are calculated from climatological aerosol.

Height and Temperature Prediction: Sensitivity of Aerosol-based CDNC

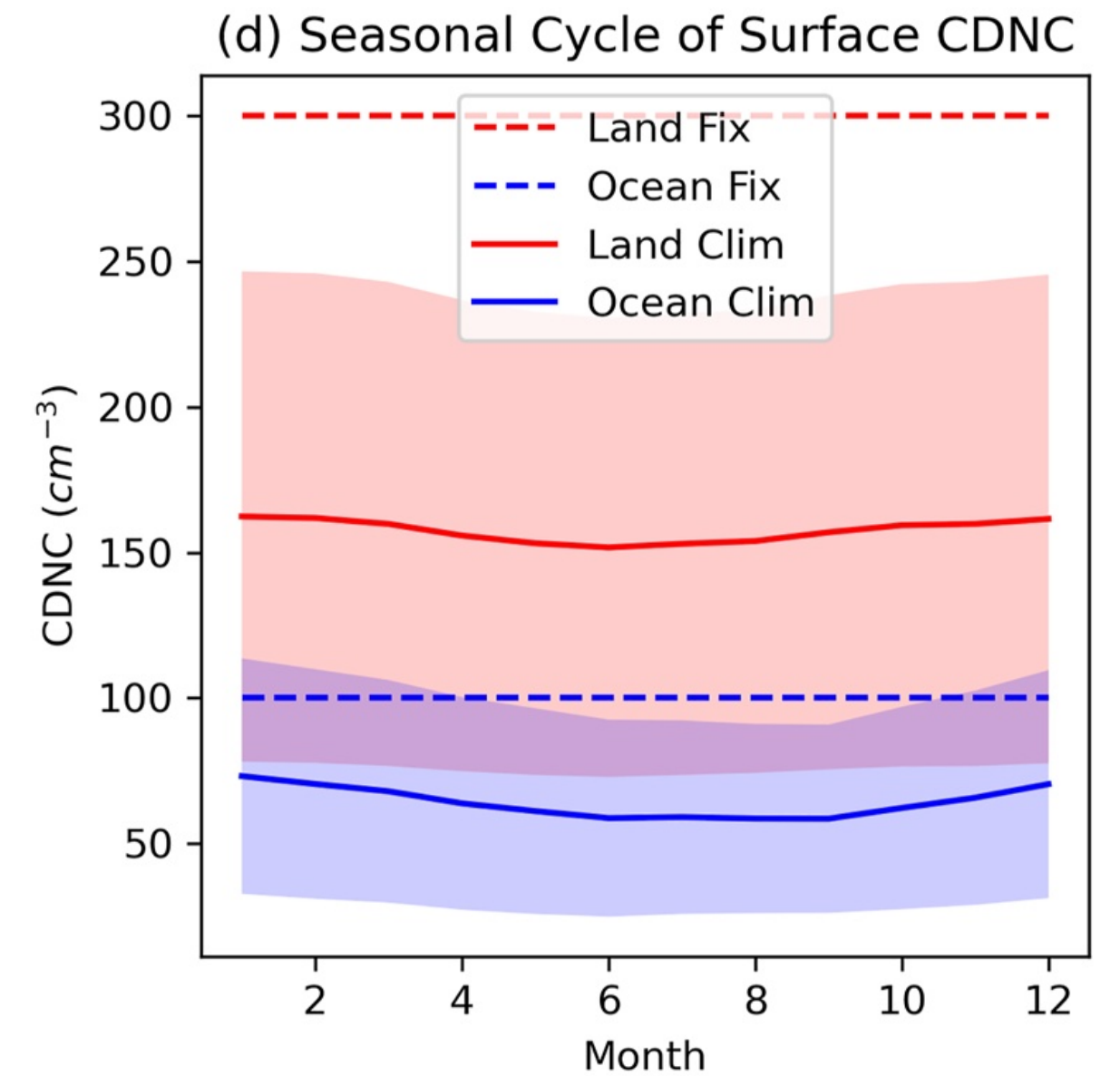
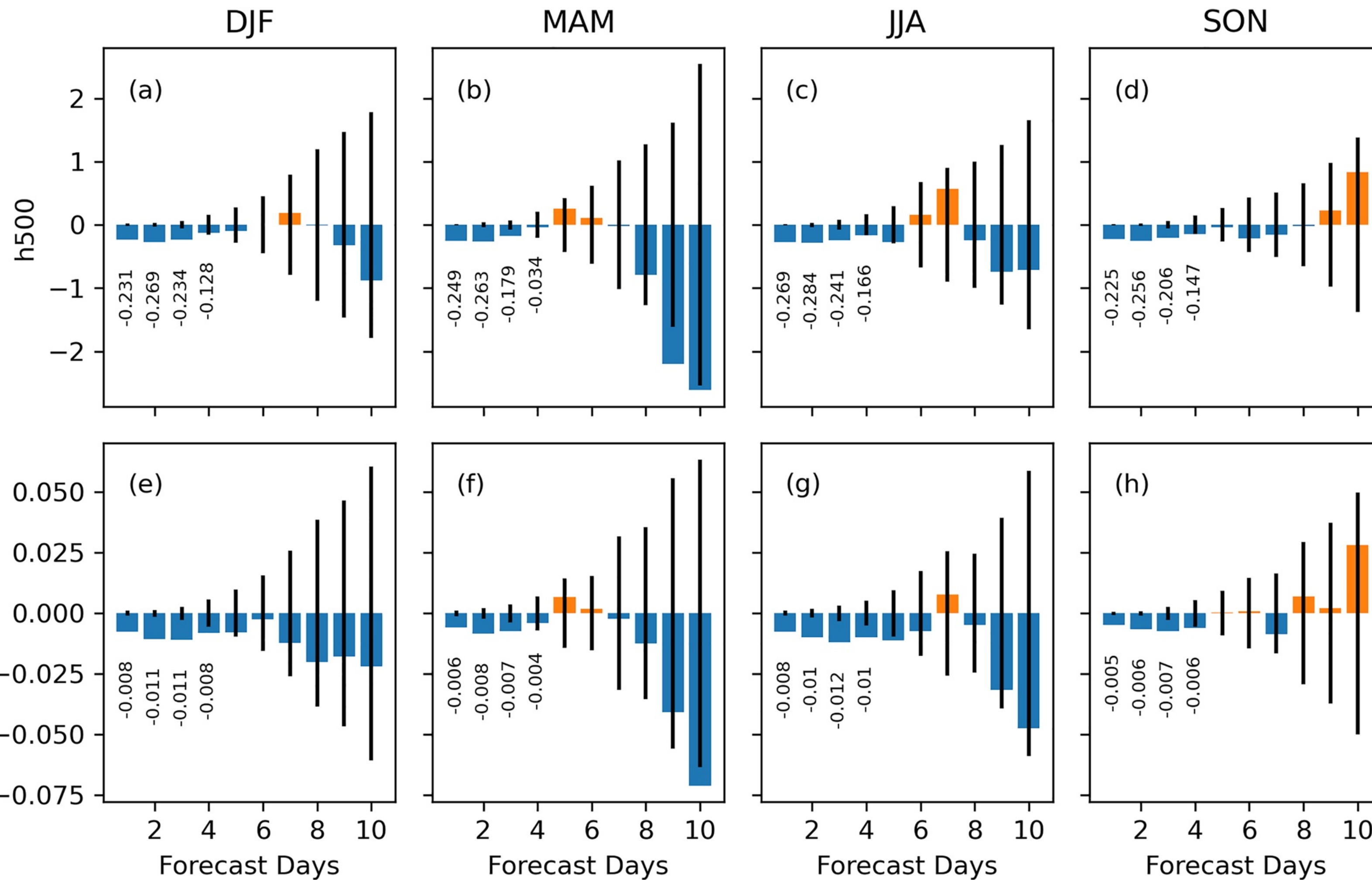


Table 2

List of Experiments in This Study

Experiment	New PSD ^a	New CDNC ^b	GFDL MP
CTRL			v3
AERO		×	v3

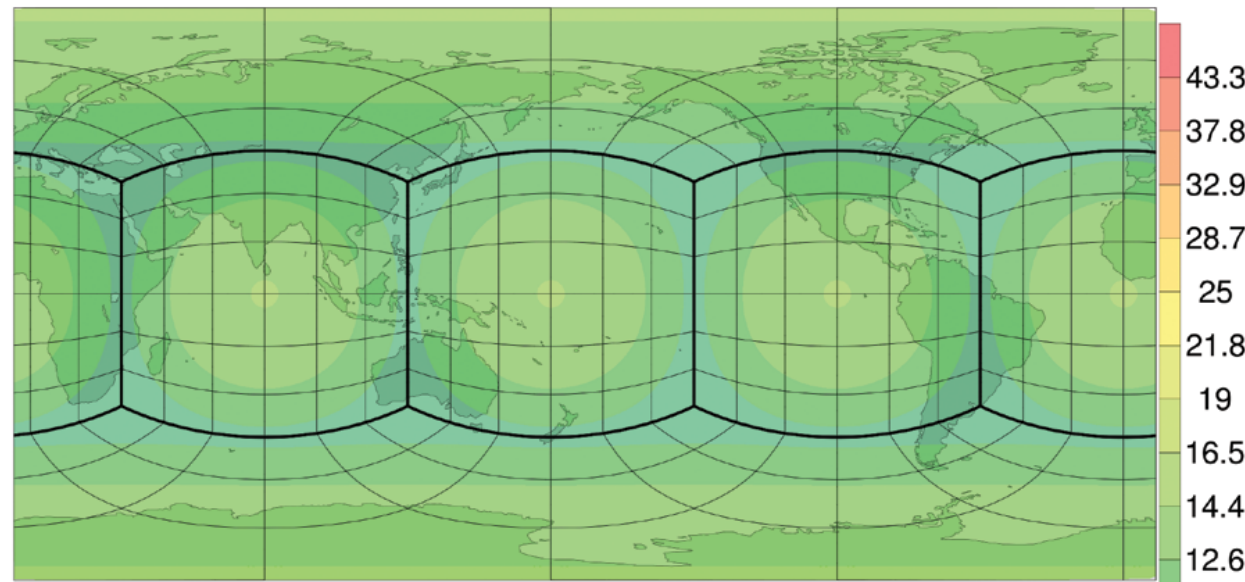
^agamma distribution for cloud water and exponential distribution for cloud ice. ^bCDNC are calculated from climatological aerosol.

Zhou et al. (2022)

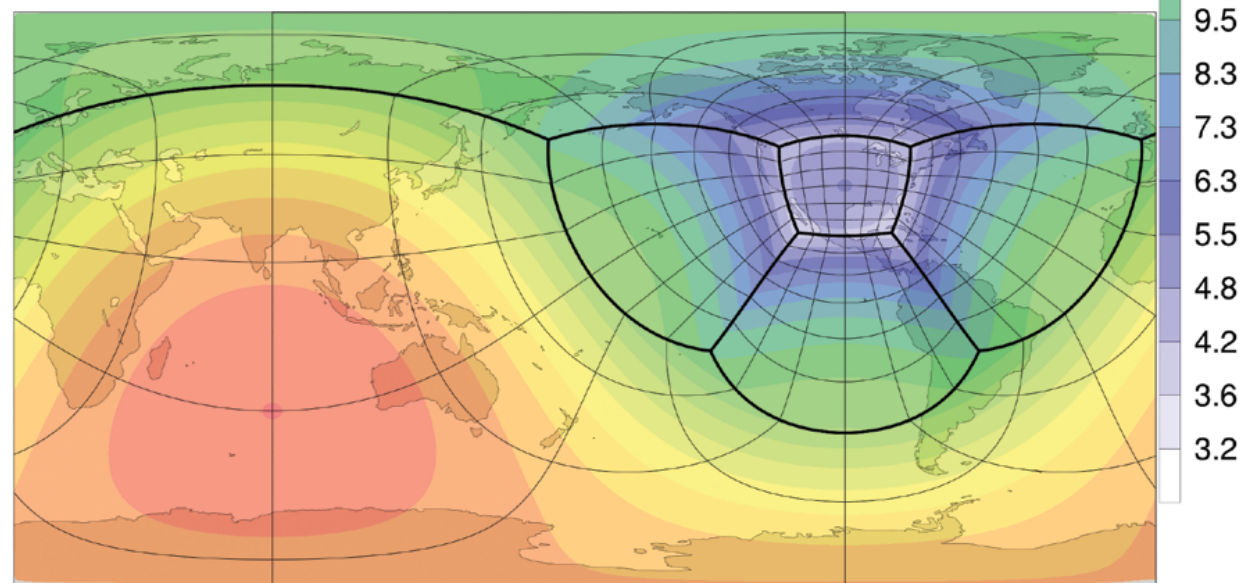
- New CDNC significantly improves H500 and T700 prediction in the first 3 days for all seasons.

Application of GFDL Microphysics in Variable-resolution SHiELD

(a) Uniform Grid, max = 14.44, min = 9.51

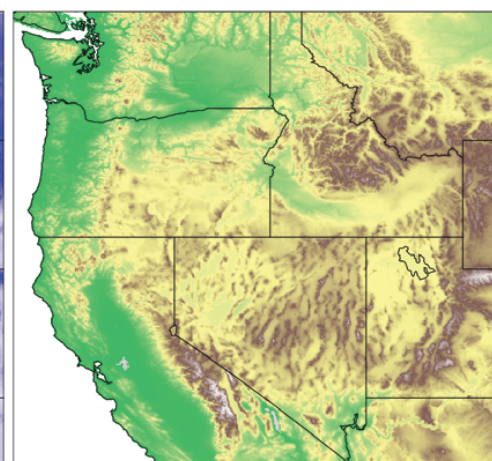
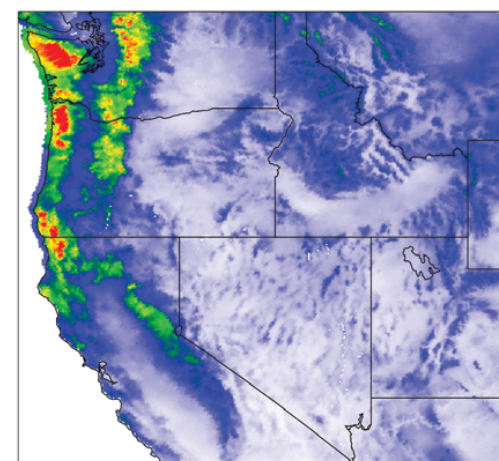


(b) Stretched Grid, max = 43.32, min = 3.9



(a) STAGEIV

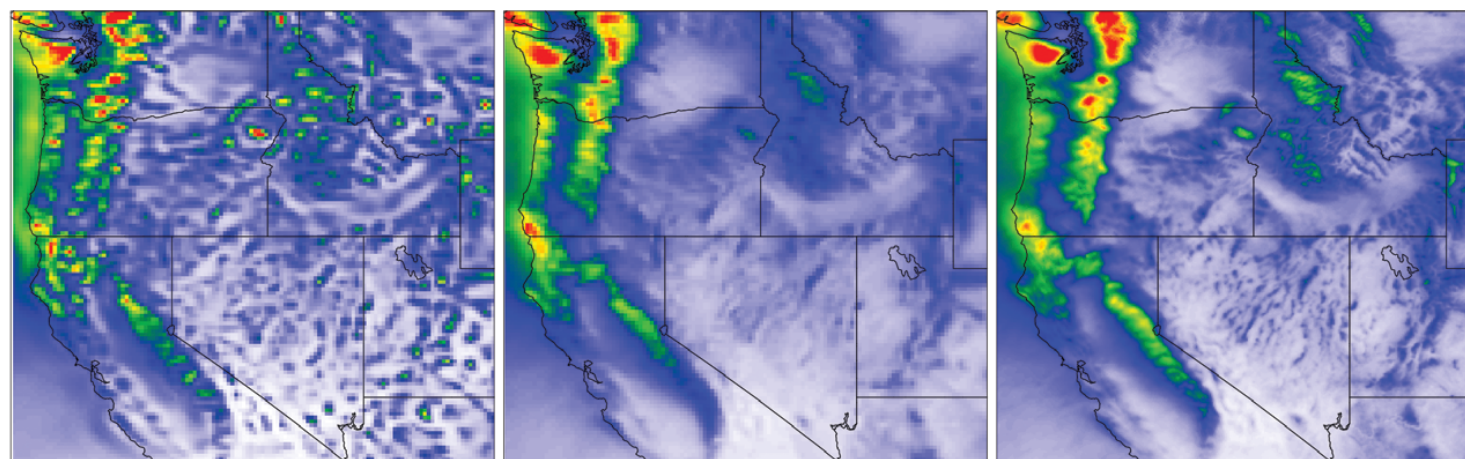
(b) Terrain



(c) GFS

(d) Uniform_ZC

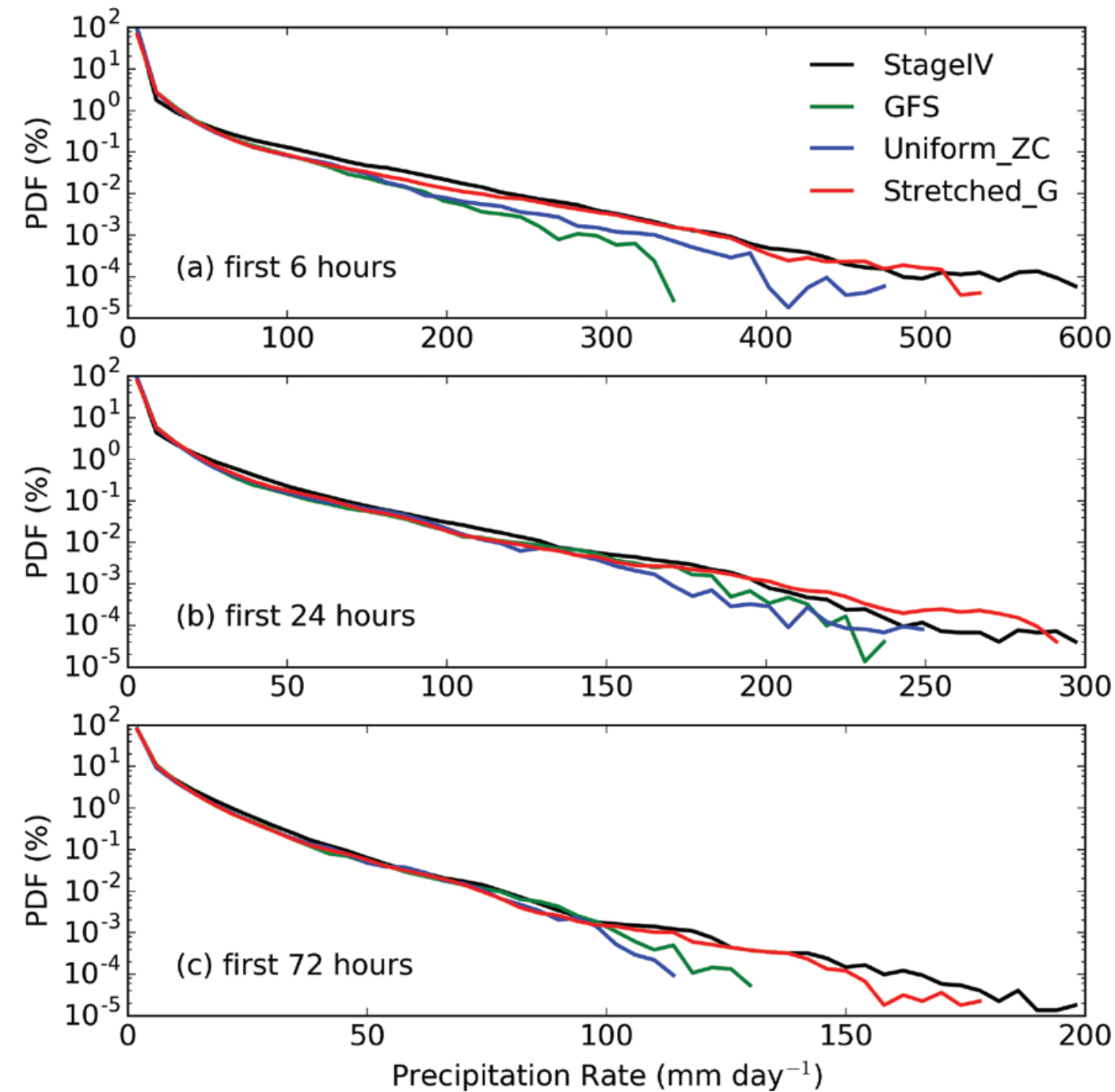
(e) Stretched_G



0.5 1 1.5 2 2.5 3 3.5 4 4.5 5 5.5 6 6.5 7 7.5 8 8.5 9 9.5 10

Zhou et al. (2019)

High-resolution CONUS, 4-45 km SHiELD

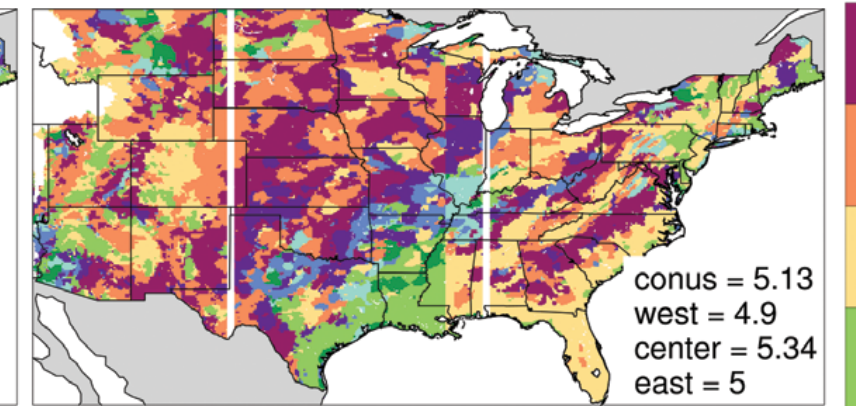
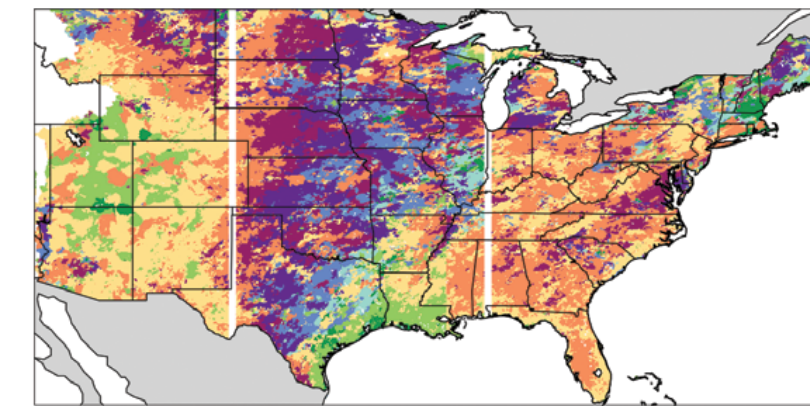


Precipitation PDF at the southern Great Plain region

West CONUS orographic precipitation

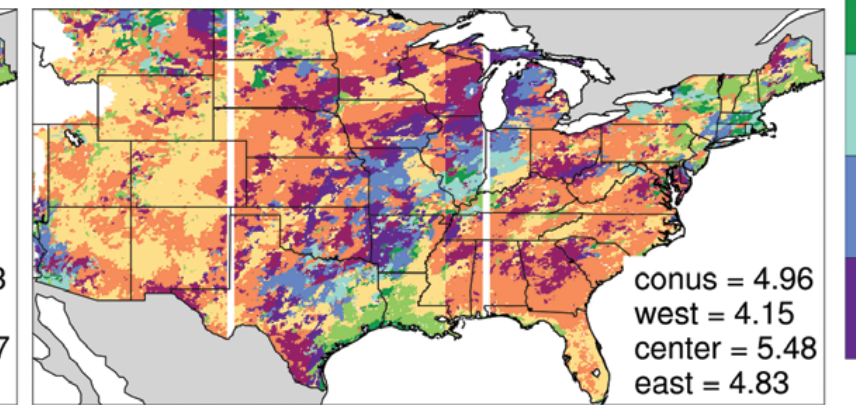
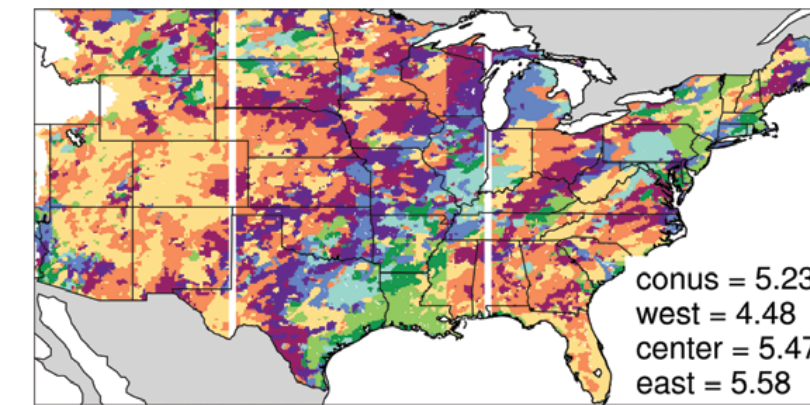
(a) StageIV

(b) GFS



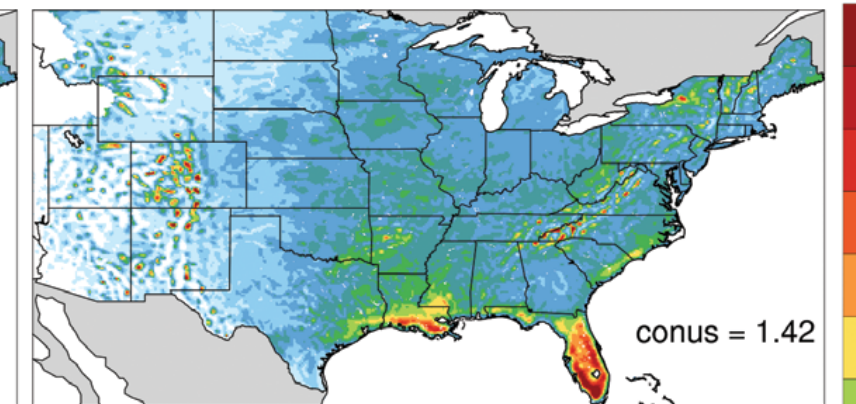
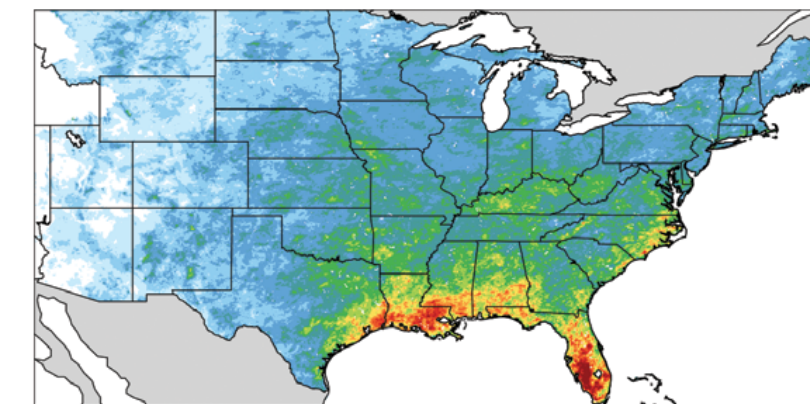
(c) Uniform_ZC

(d) Stretched_G



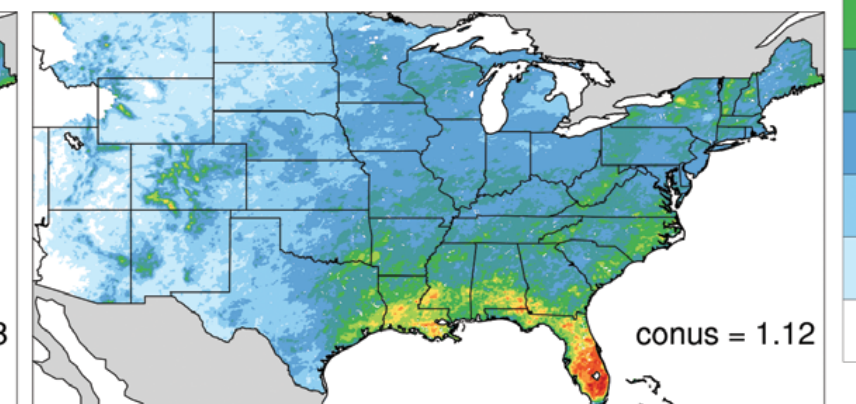
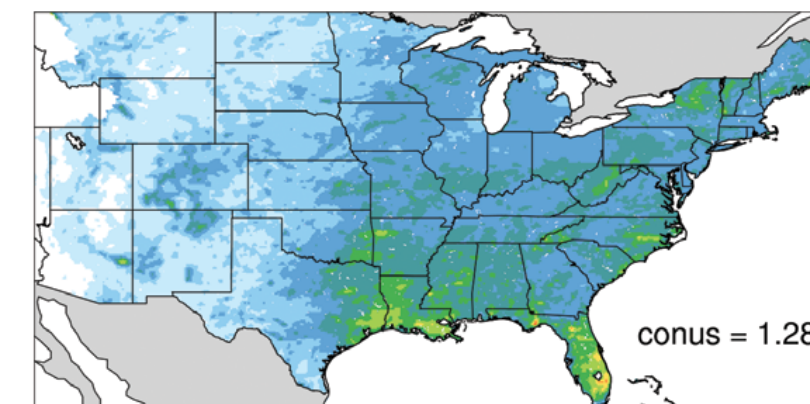
(e) StageIV

(f) GFS



(g) Uniform_ZC

(h) Stretched_G



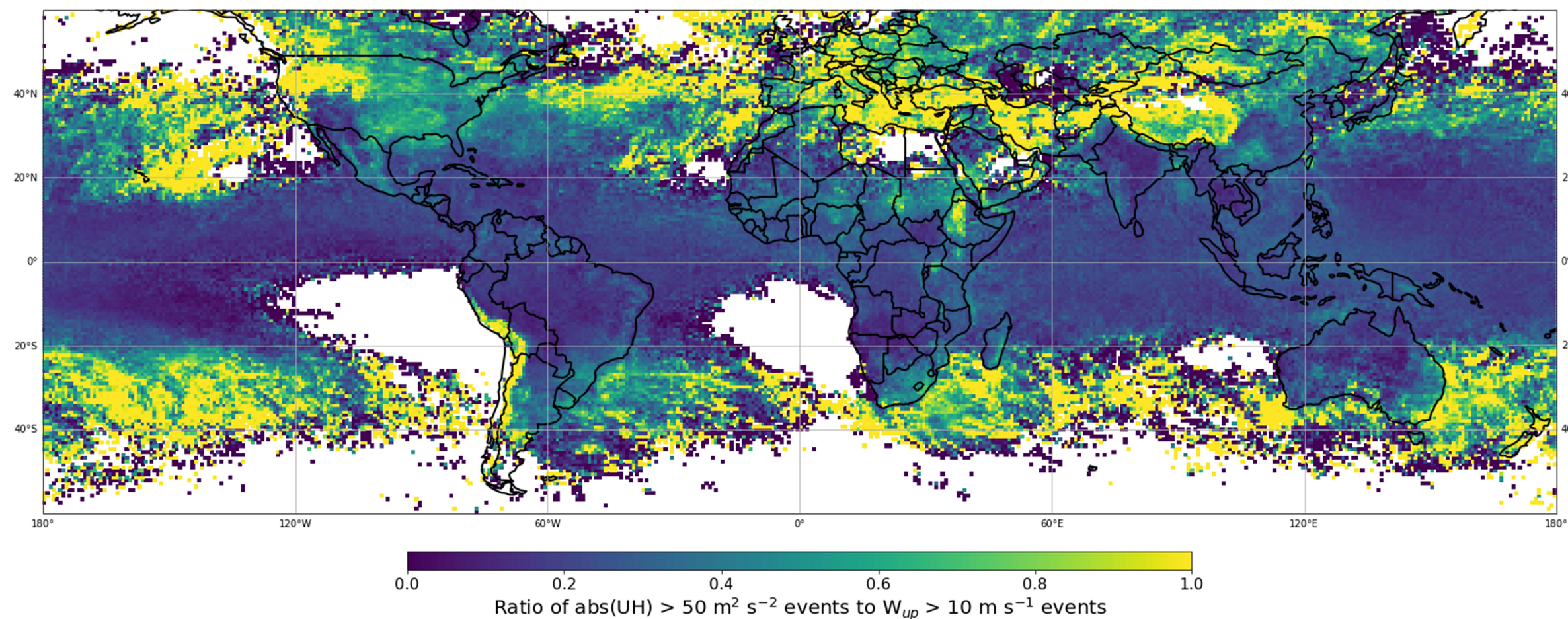
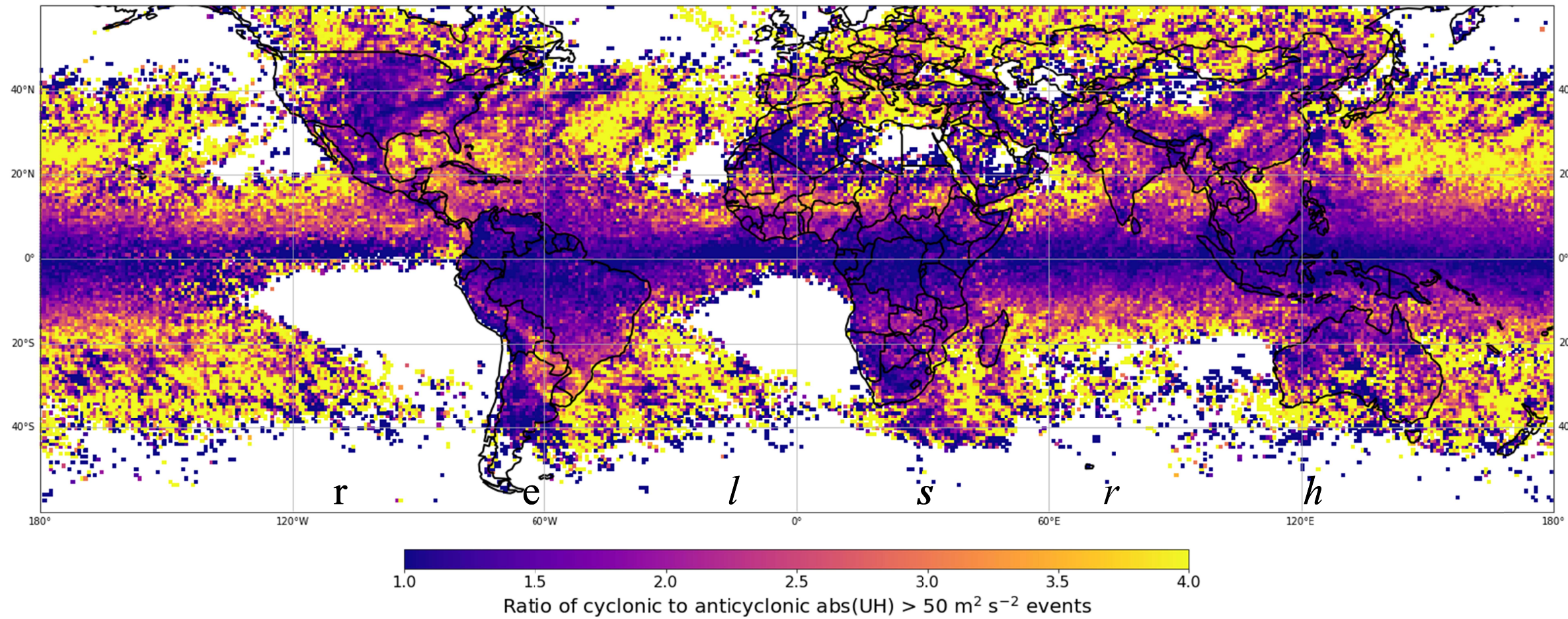
(g) Uniform_ZC

(h) Stretched_G

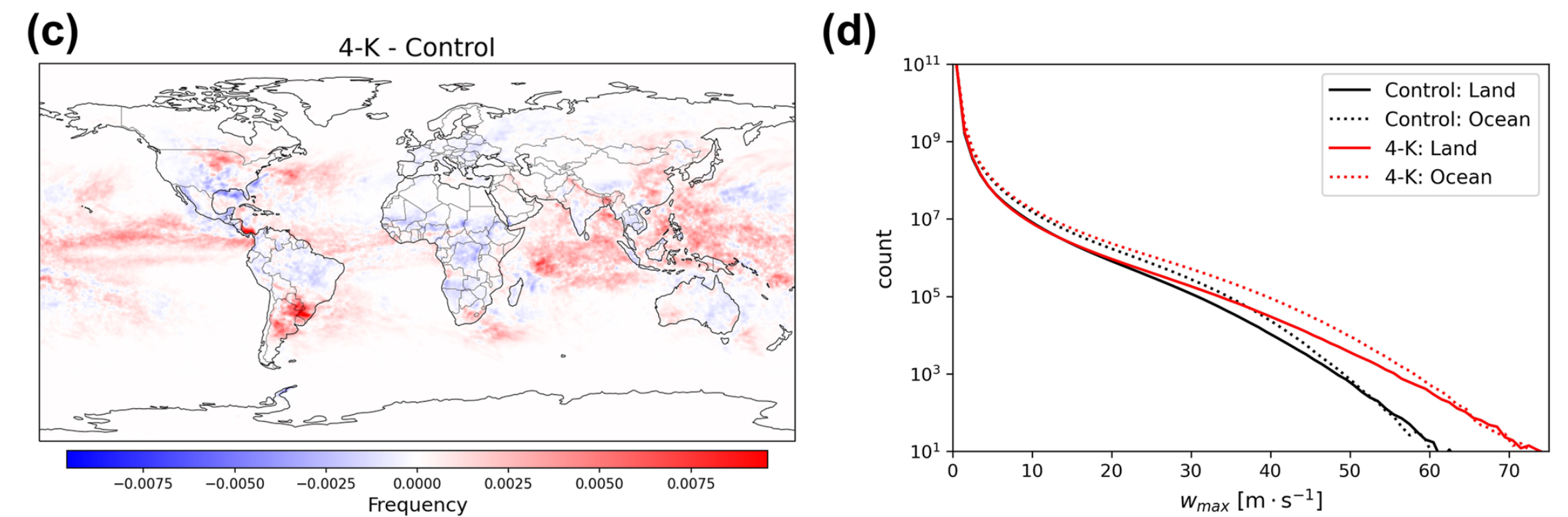
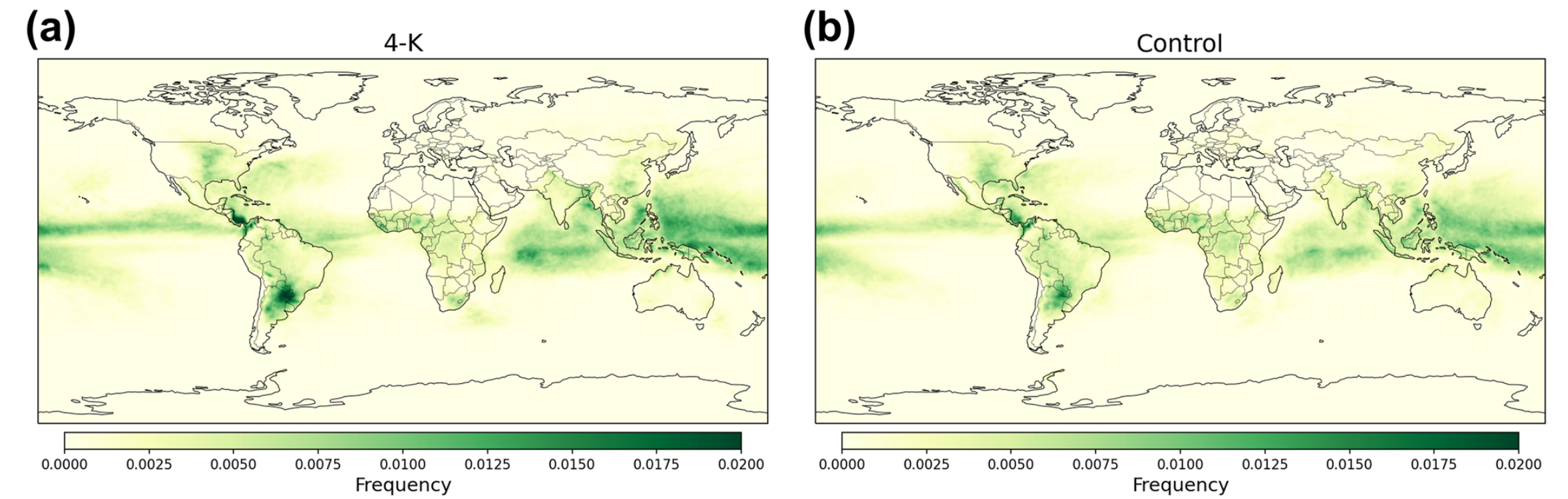
Precipitation peak time and amplitude

- High-resolution enables convective-scale prediction
- GFDL Microphysics is capable of predicting intense precipitation, and it handles the diurnal cycle well

GFDL Storm-resolving Model X-SHiELD



Harris et al. (2023)



Cheng et al. (2022)

Year-long global storm prediction:

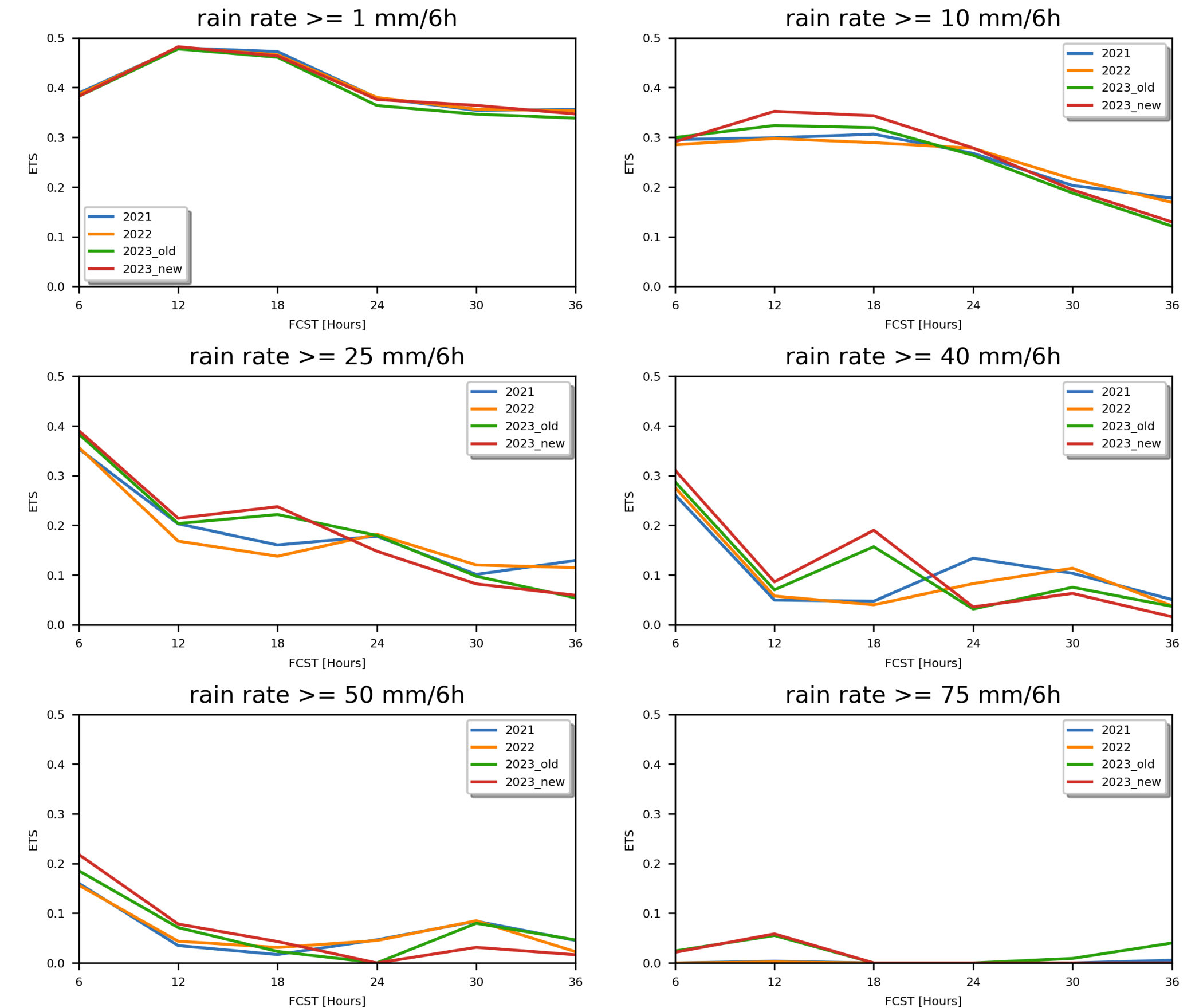
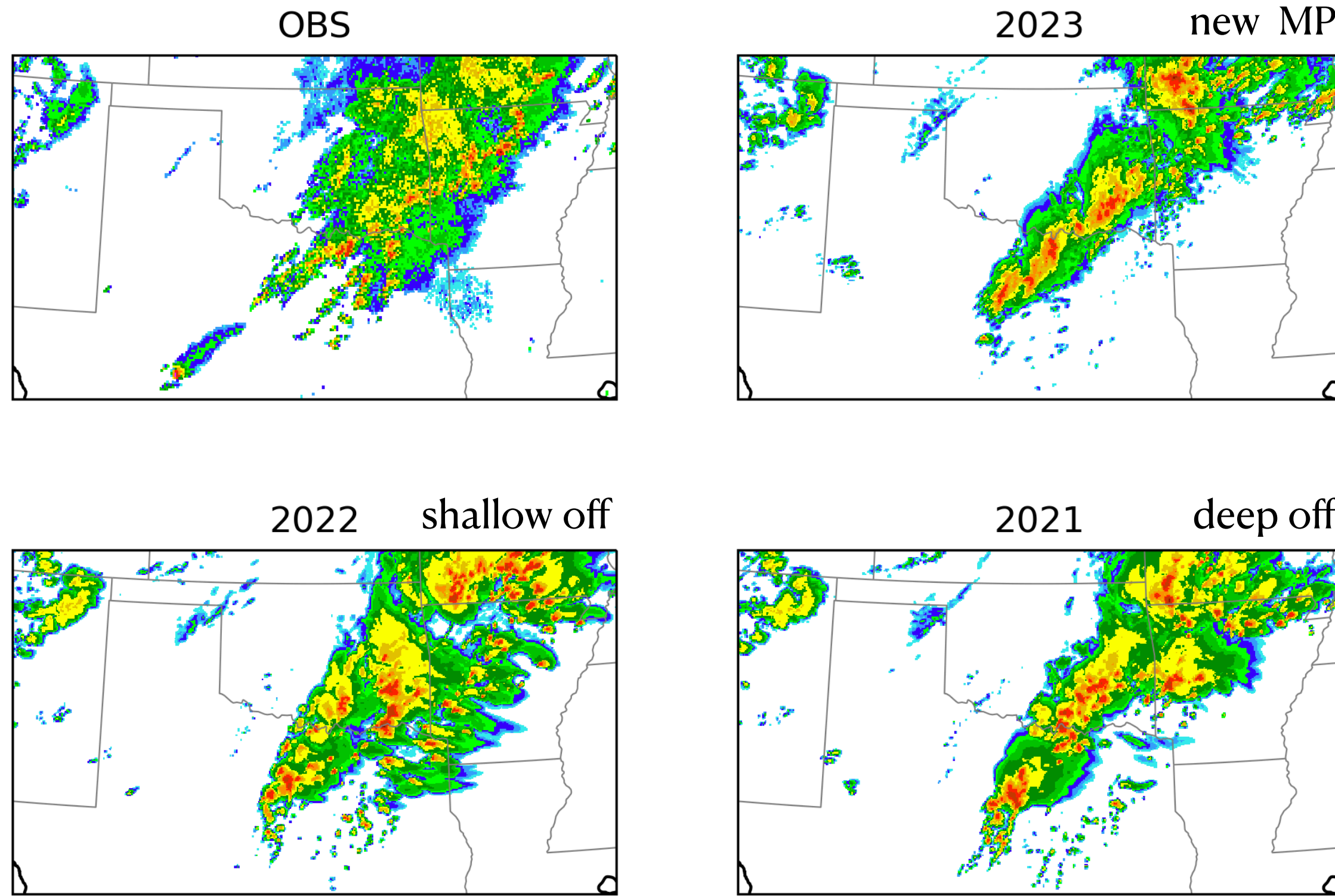
- More cyclonic rotations appear farther away from the equator
- More rotations are in the subtropics & mid-latitudes in intense updrafts

In warming scenario:

- The annual occurrence of intense convection increases by 21%
- The most extreme vertical velocities increase by about 20%
- The ocean becomes more favorable for intense convection
- Intense continental convection moves poleward

Microphysics Development for C-SHiELD

2019052921Z (Fcst hour: 21)



Courtesy of Kai-Yuan Cheng

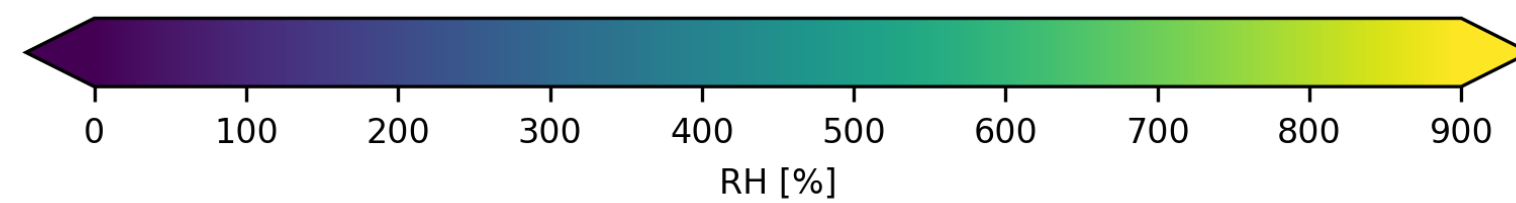
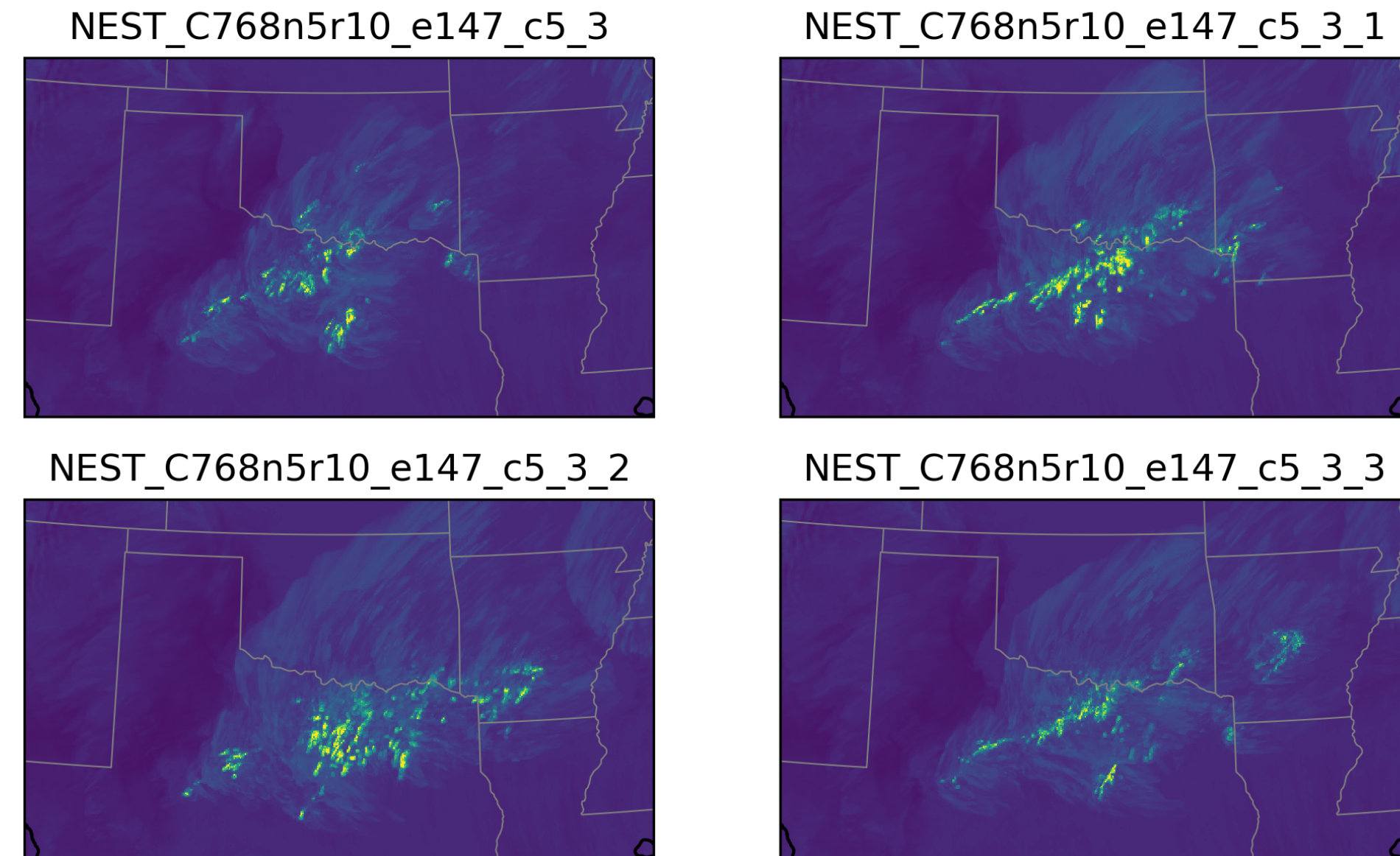
Microphysics Updates:

1. Condensation and evaporation are done at the last cycle of vertical remapping \rightarrow reduce intense and fast moving organized convections
2. Saturation adjustment is added to the end of all physical parameterizations \rightarrow reduce supersaturation

Microphysics Development for C-SHiELD

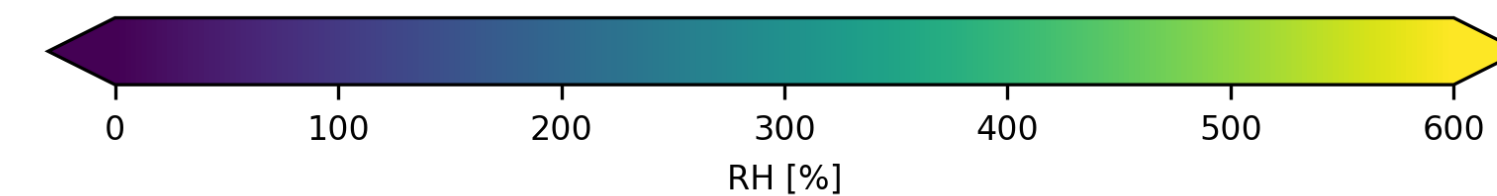
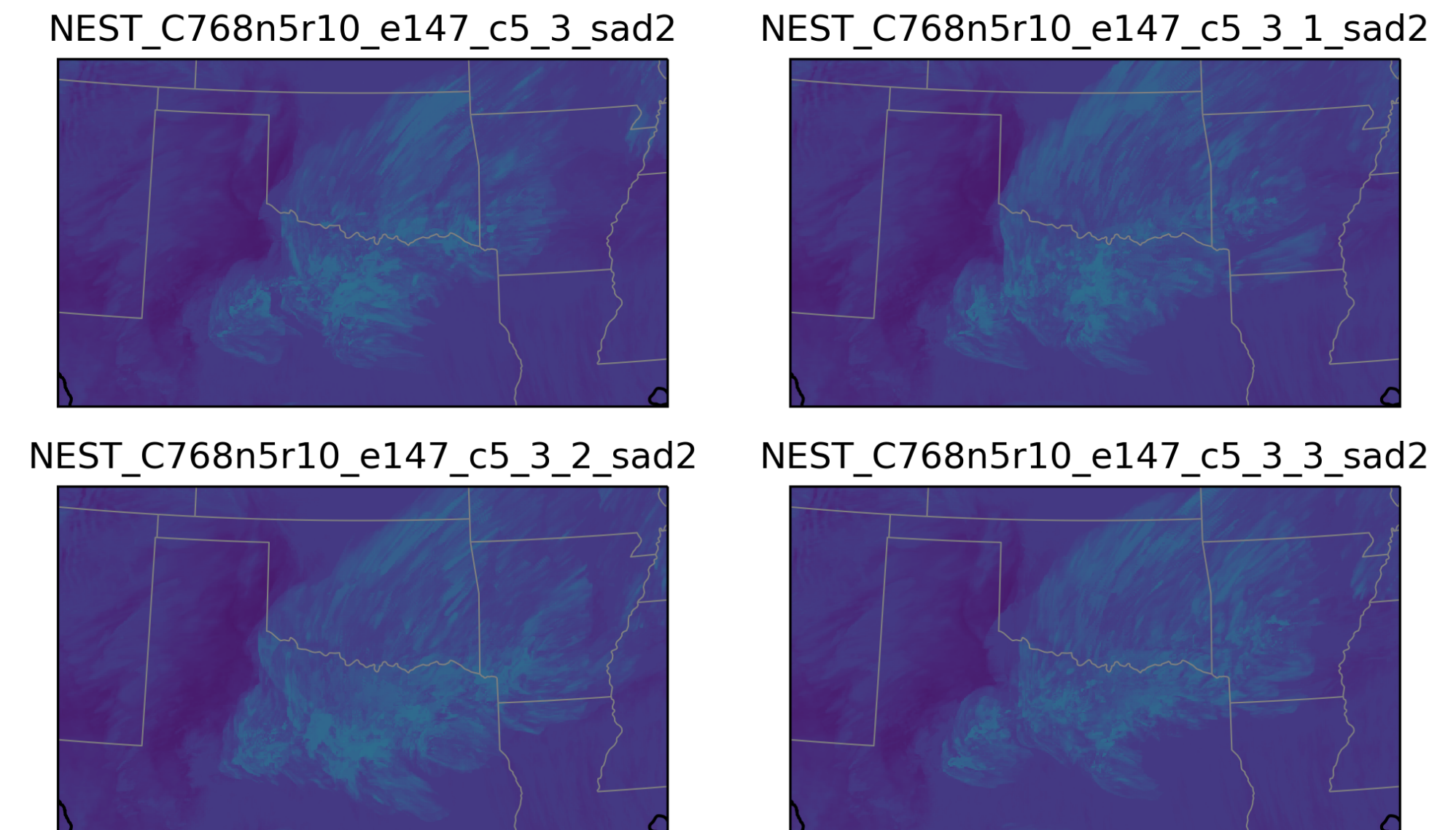
Inline GFDL MP

2019050200Z (Fcst hour: 24)



Inline GFDL MP + Saturation Adjustment

2019050200Z (Fcst hour: 24)



Courtesy of Kai-Yuan Cheng

Microphysics Updates:

1. Condensation and evaporation are done at the last cycle of vertical remapping → reduce intense and fast moving organized convections
2. Saturation adjustment is added to the end of all physical parameterizations → reduce supersaturation

Microphysics Development for C-SHiELD

Split GFDL MP

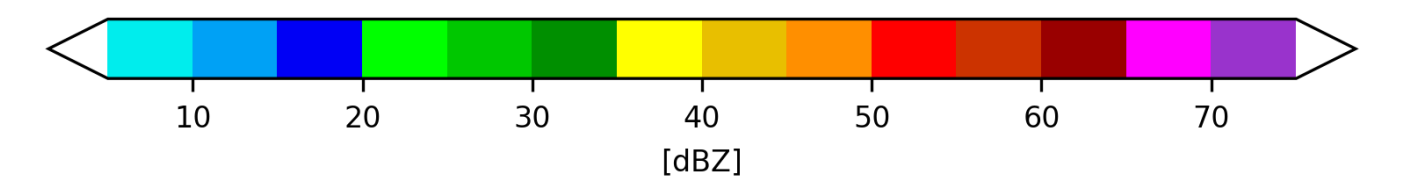
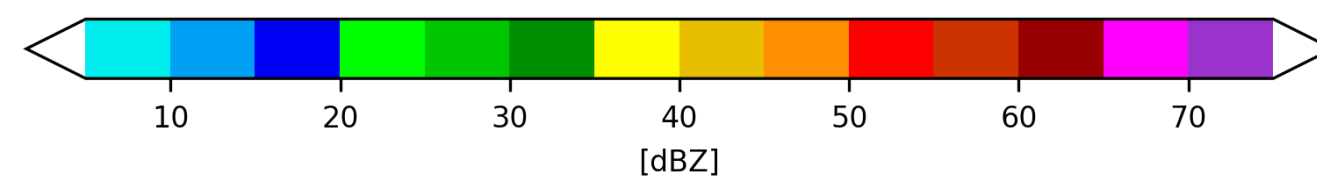
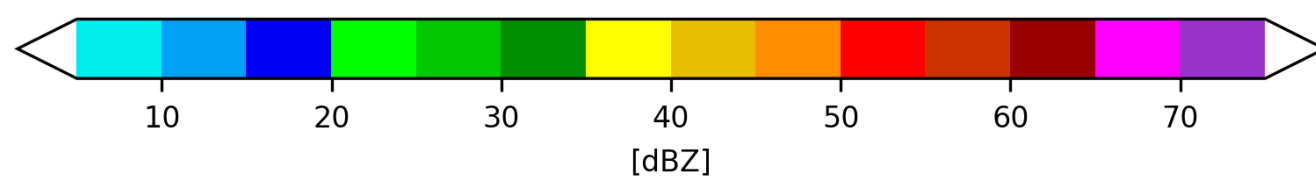
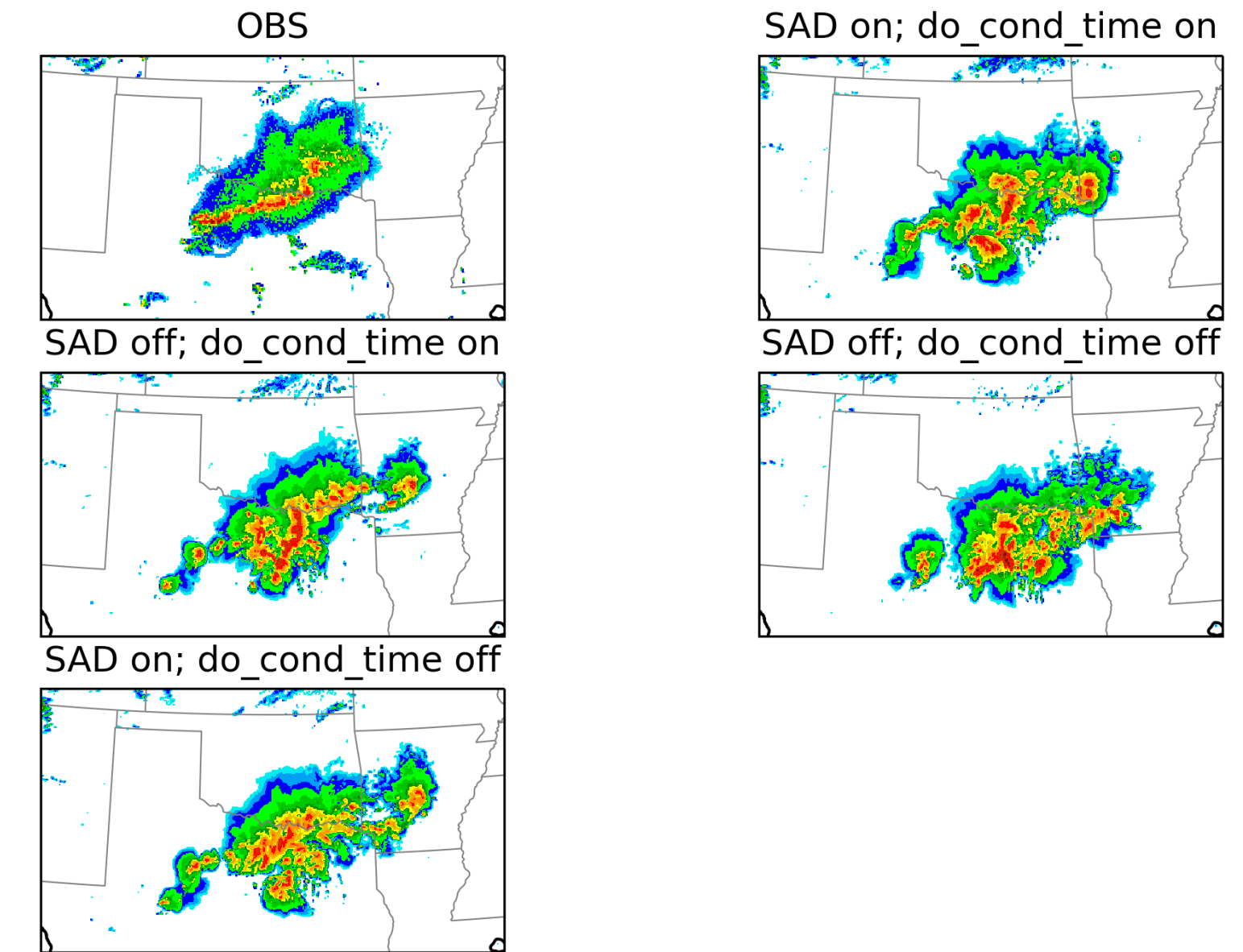
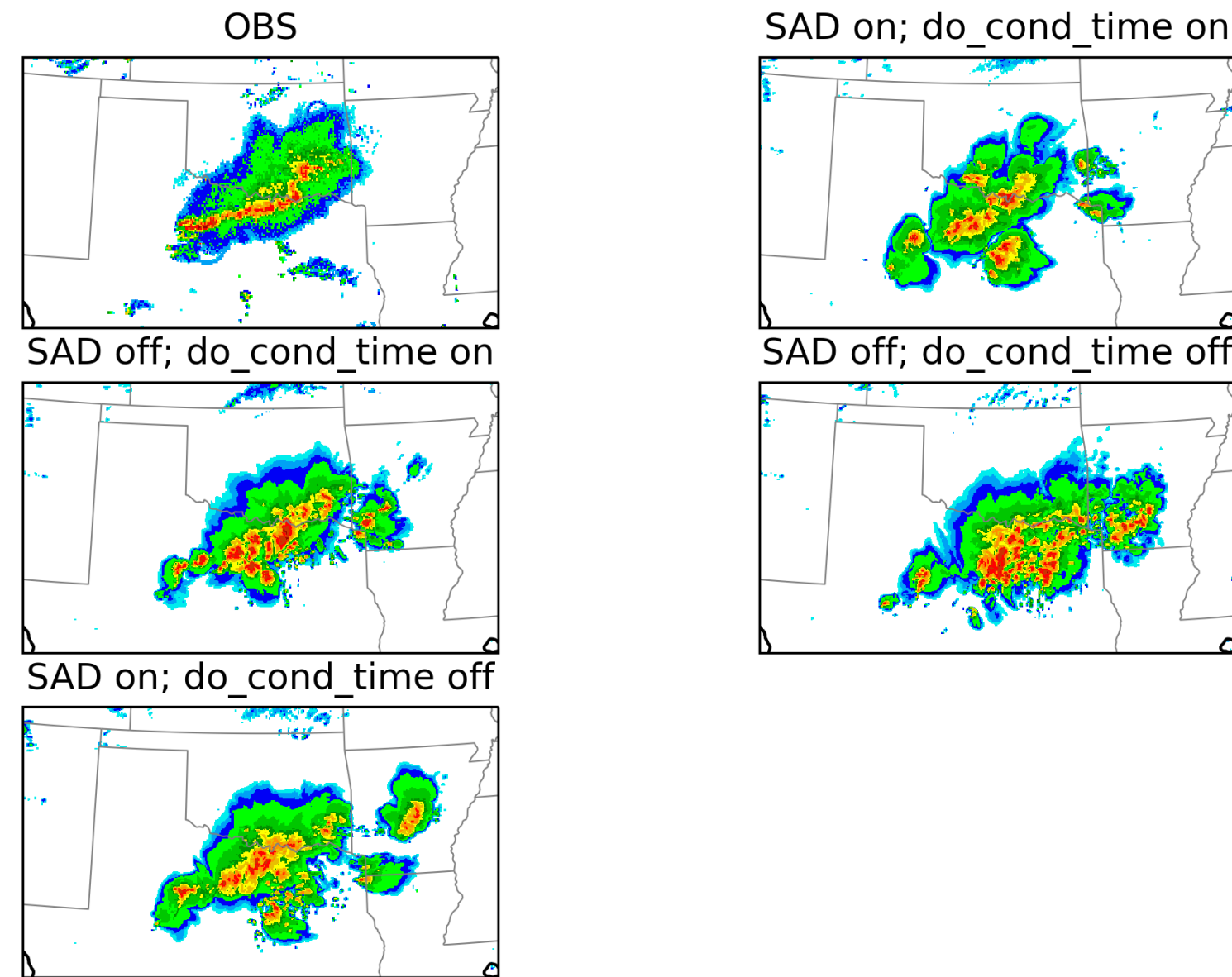
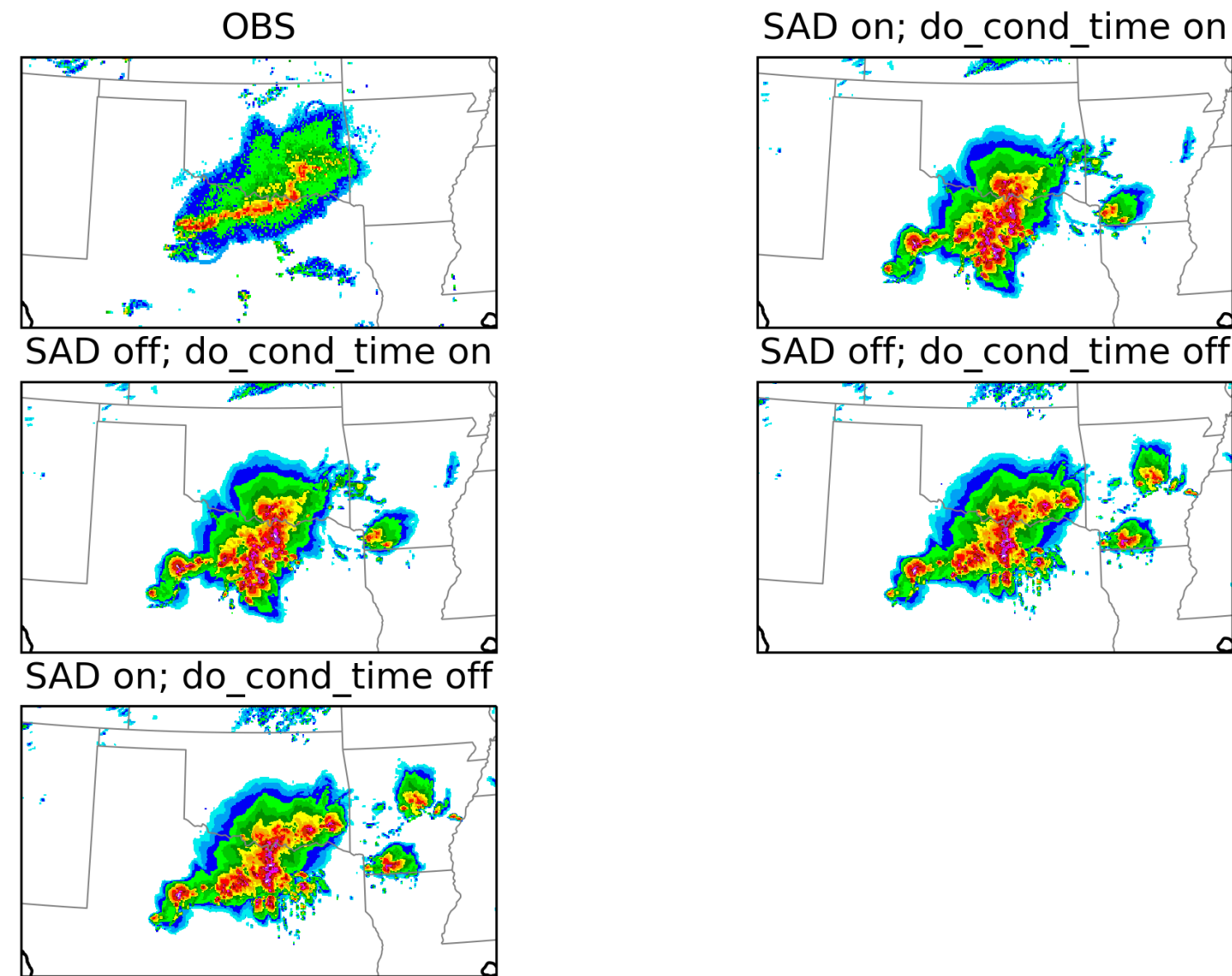
Inline GFDL MP

Inline GFDL MP + Saturation Adjustment

2019050200Z (Fcst hour: 24)

2019050200Z (Fcst hour: 24)

2019050200Z (Fcst hour: 24)



SAD: Saturation Adjustment Delay

Courtesy of Kai-Yuan Cheng

Microphysics Updates:

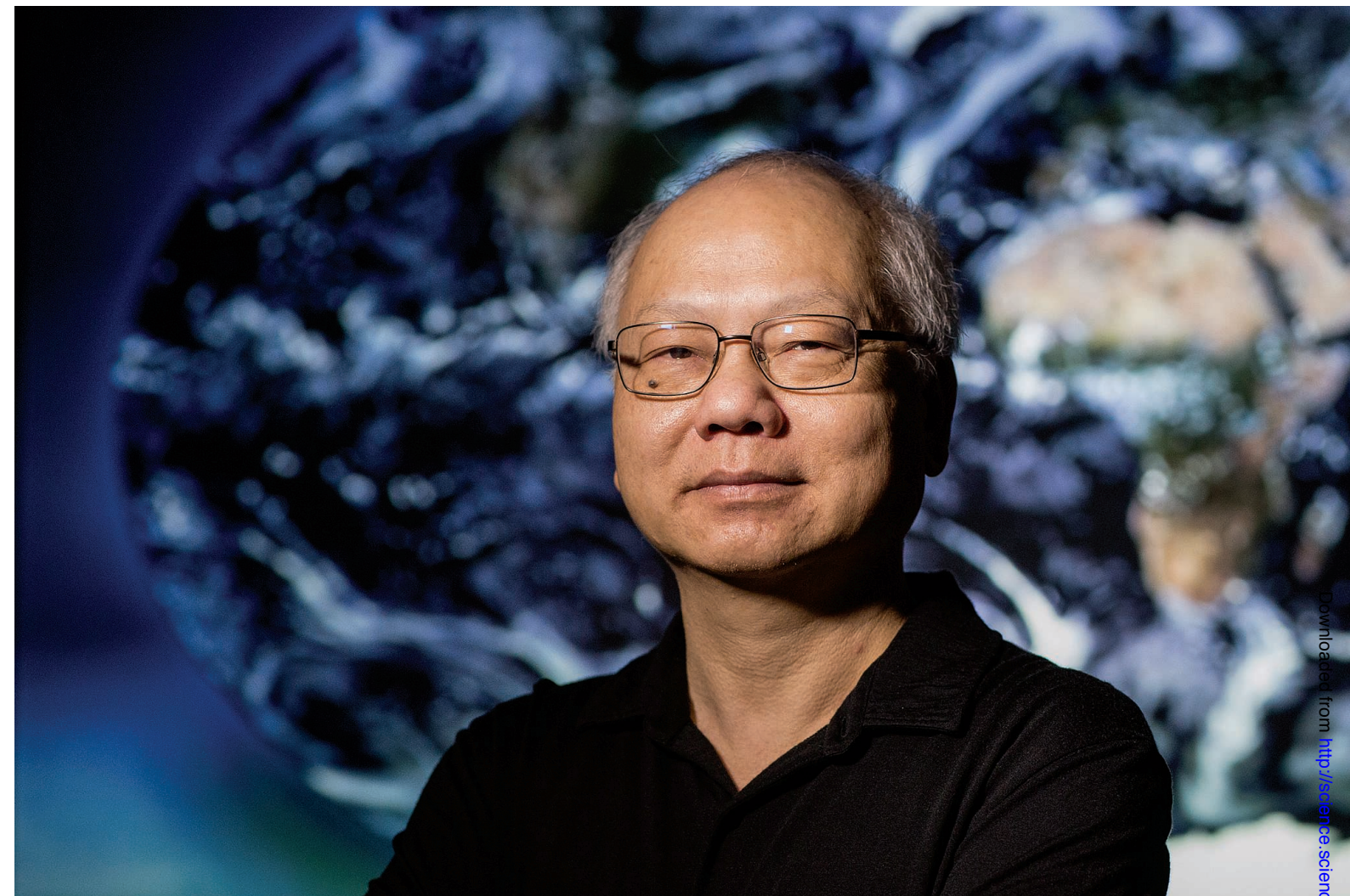
1. Condensation and evaporation are done at the last cycle of vertical remapping → reduce intense and fast moving organized convections
2. Saturation adjustment is added to the end of all physical parameterizations → reduce supersaturation



PRINCETON
UNIVERSITY



Allen Institute for AI



THE WEATHER MASTER

How Shian-Jiann Lin's atmospheric grids could unify weather forecasts and climate models

By Paul Voosen

Downloaded from <http://www.sciencemag.org/> on October 4, 2019



S.-J. Lin (retired) and the GFDL FV3 Team (now)